EE 502: Microwave Engineering

Dr. Dennis Derickson

79 GHz Multiport Amplifier and Antenna System

Pavin S. Virdee

March 18, 2021

Electrical Engineering Department

California Polytechnic State University, San Luis Obispo

Contents

List of Figures

List of Tables

1 Introduction

The objective of this term project is to design a multi-port amplifier and antenna system for a millimeter wave 5G band with dynamic control over power distribution and beam-steering.

The application of this design was chosen to be for Automotive Radar applications operating within the new state-of-the-art 77 GHz radar band. This 77 to 81 GHz band is within the IEEE defined W-band and serves as the new short-range radar band replacing the legacy 24 GHz band [5]. This new band boasts larger available bandwidths and better resolutions, smaller physical size, and higher power levels [6], all advantages behind the shift up to the 77 GHz band from the 24 GHz band. *This design will specifically focus on a center frequency of 79 GHz.*

Multi-port Amplifier's can be implemented in a similar fashion as phased-array antenna systems. They allow for dynamic, directional control over power, bandwidth, and beam-forming capability. Using an MPA system for automotive radar application can be advantageous with up-and-coming autonomous driving solutions. Figure 1 below shows how controlling the phase of each antenna's propagating wave can control where the transmitted field and wave will be the strongest due to constructive and destructive wave interference as well as dynamic power control. This allows the direction and power of the transmitted wave (or beam) to be steered (by θ° of Figure 1) by manipulating the respective phase of each ports propagated signal. In automotive radar applications this can allow for more efficient signal and power distribution in regard to environmental sensing and autonomous driving.

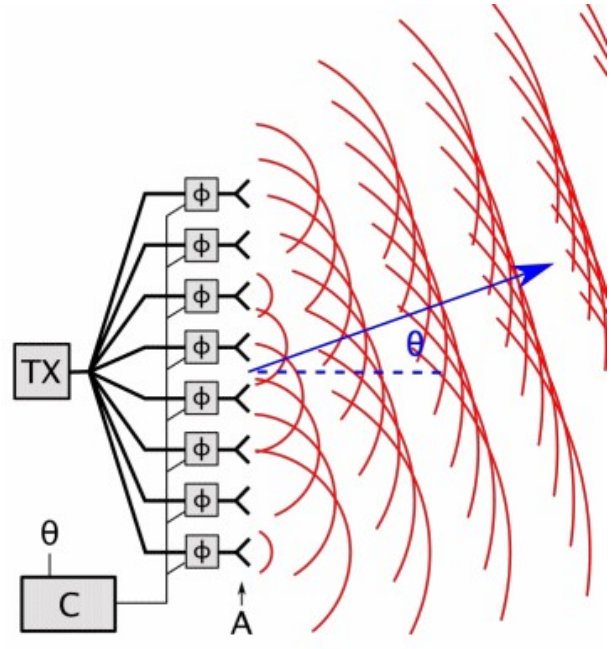

Figure 1: Antenna Array Beam-Steering and Power Distribution Diagram (*reference 'Phased Array' via The Free Encyclopedia)*

2 Specifications and Requirements

Table 1 below shows the initial design specifications and requirements for this term project. Note that the TX signal direction is in units *degrees* and is equivalent to the θ angle in Figure 1.

Table 1: Design Specifications and Requirements

Parameter	Min	Typ	Max	Unit
Operational Frequency	77	79	81	GHz
System Gain	10	-	-	dB
Operating Voltage	-	4.0	-	V
TX Signal Direction	-50	-	+50	°
Single Port Focused Output Power	75	-	-	W
Four Port Balanced Output Power	25	-	-	W
DC Power Consumption	-	-	700	mW

3 Block Diagram

A full system level block diagram is shown below in Figure 2. The system features butler matrices on the input and output system ends, four 50 Ω matched amplifiers, four TX antennas, four respective phase shifters, and several matching networks. The initial design for the phase shifter will be simply utilizing transmission lines and varying the length to vary the propagation delay and relative phase shift.

The amplifier block has also been selected to be the HMC-AUH320 GaAs HEMT MMIC Medium Power Amplifier [3] and is discussed in Section 4. The quadrature couplers will represent 90° Hybrid couplers and the antennas will either be selected or designed. Several other system components are discussed in the following sections.

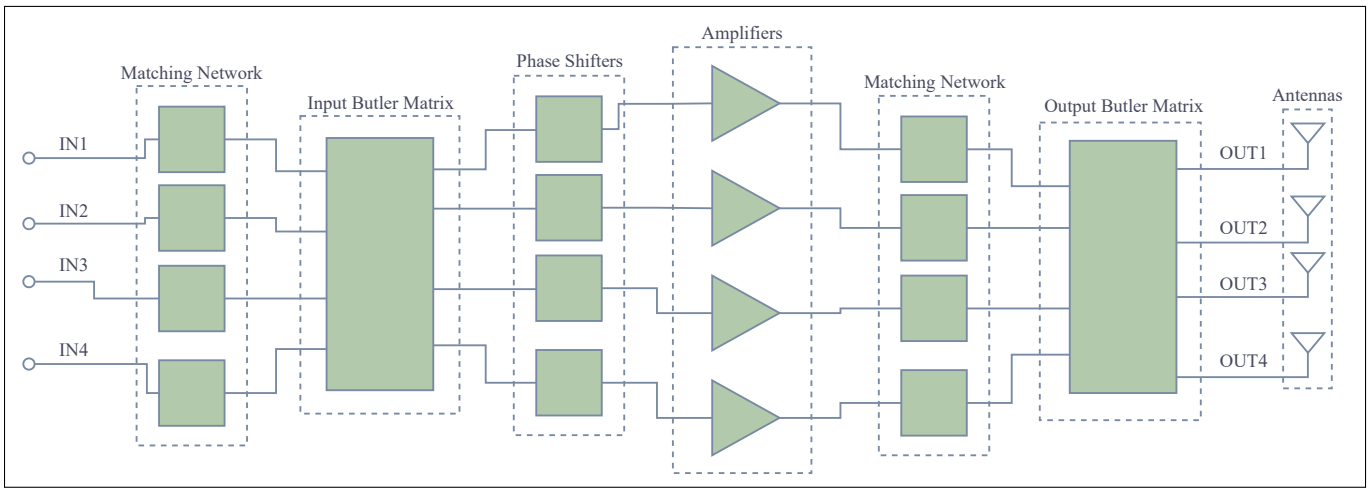

Figure 2: System Block Diagram

4 Amplifiers

The amplifier device serves as one of the most important components of this design. Arranging four amplifiers in a balanced topology allows for the combination and potential of quadrupling output power at a single, given output port.

A search for a suitable amplifier was conducted to find one with acceptable performance specifications to satisfy the given system design specifications.

4.1 Device Selection and Initialization

Gain, bandwidth, power consumption, and dynamic range measurements were all considered when selecting an amplifier. Another factor that was important was confirming that the amplifier either had a transistor model to be imported into ADS or available S2P files including Scattering Parameters. Without one of these two options, it would be impossible to model and simulate the amplifier in ADS.

After exploring several options, the HMC-AUH320 GaAs HEMT MMIC Medium Power Amplifier, by Analog Devices was selected. It was chosen for its considerable gain, high dynamic range, and low power consumption all within the frequency band of operation. Table 2 below highlights the electrical specifications of the HMC-AUH320 amplifier.

Table 2: HMC-AUH320 Amplifier Performance Specifications [3]

Parameter	**Min**	**Typ**	**Max**	**Unit**
Frequency Range	71	-	86	GHz
Gain	10	16	-	dB
Input Return Loss	-	4	-	dB
Output Return Loss	-	6	-	dB
1dB Compression Output Power (P1dB)	-	15	-	dBm
Saturated Output Power (P_{sat})	-	16	-	dBm
Supply Current	-	130	-	mA
Supply Voltage	-	4	-	V
Input/Output Impedance	-	50	-	Ω

4.2 Amplifier Performance

A model for the selected amplifier can now be created in ADS. Since a S2P file was provided by Analog Devices, the file can simply be imported into a SNP block within ADS to model the device. Pins can be attached to the input and output of the SNP block respectively, as seen in Figure 3.

An amplifier symbol was then created from the schematic shown in Figure 3 utilizing ADS's hierarchical network feature [7]. Figure 4 highlights the HMC-AUH320 ADS symbol used for the design.

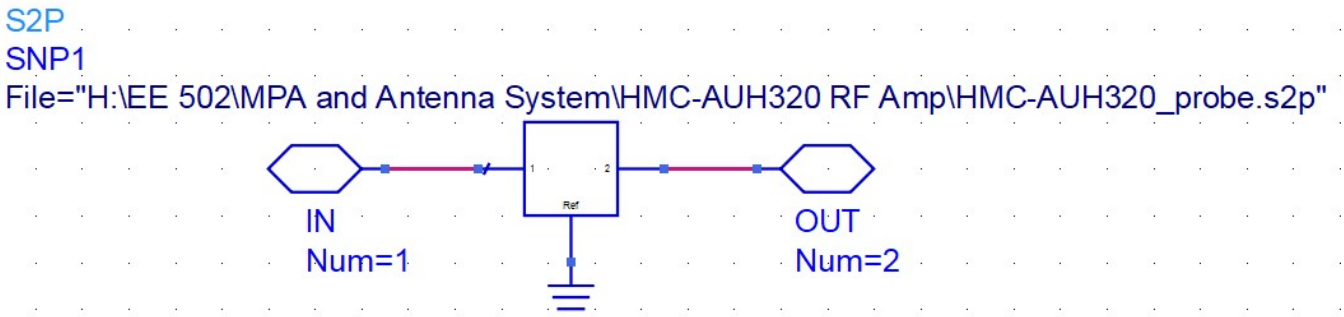

Figure 3: HMC-AUH320 Amplifier Sub-Symbol (internal) Schematic

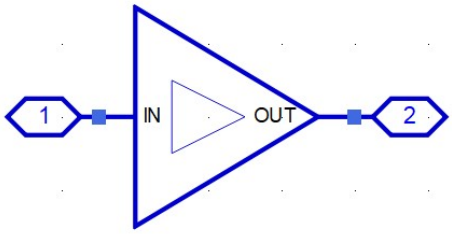

Figure 4: HMC-AUH320 Amplifier Symbol

An S-Parameter simulation can then be performed on the device to verify that the amplifier is performing to the specifications noted in Table 2 (and the datasheet [3]).

Figure 5 below displays the schematic used to perform a S-Parameter simulation on the amplifier from 77 to 81 GHz. Figure 6 highlights all four S-Parameter results.

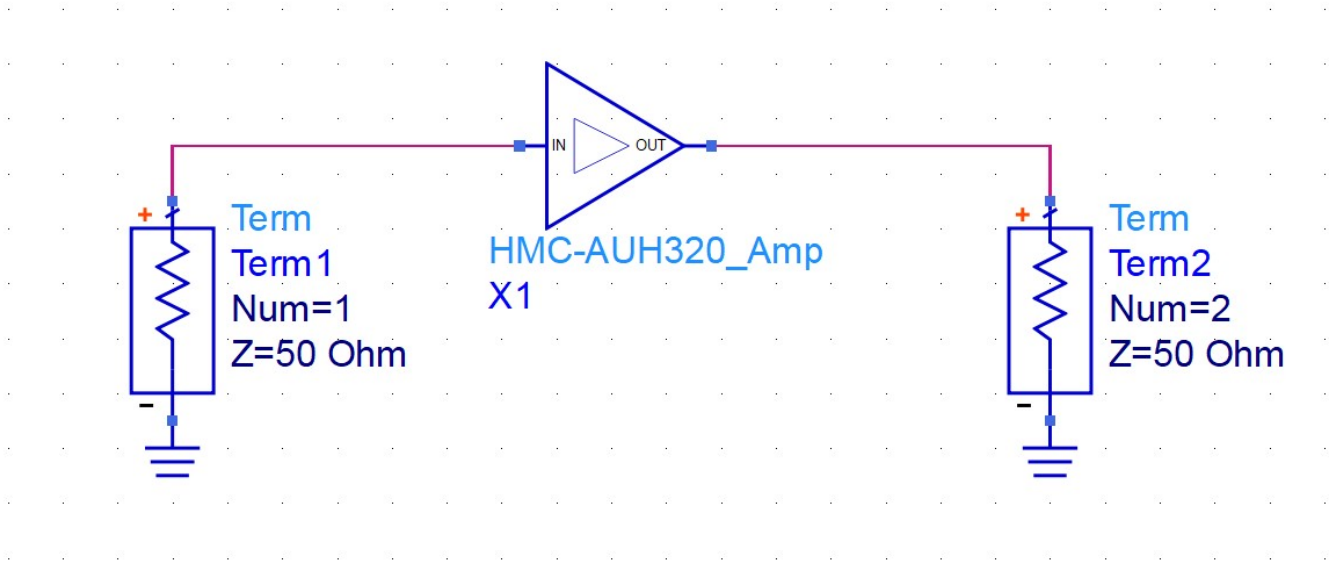

Figure 5: HMC-AUH320 RF Performance Verification Test Schematic

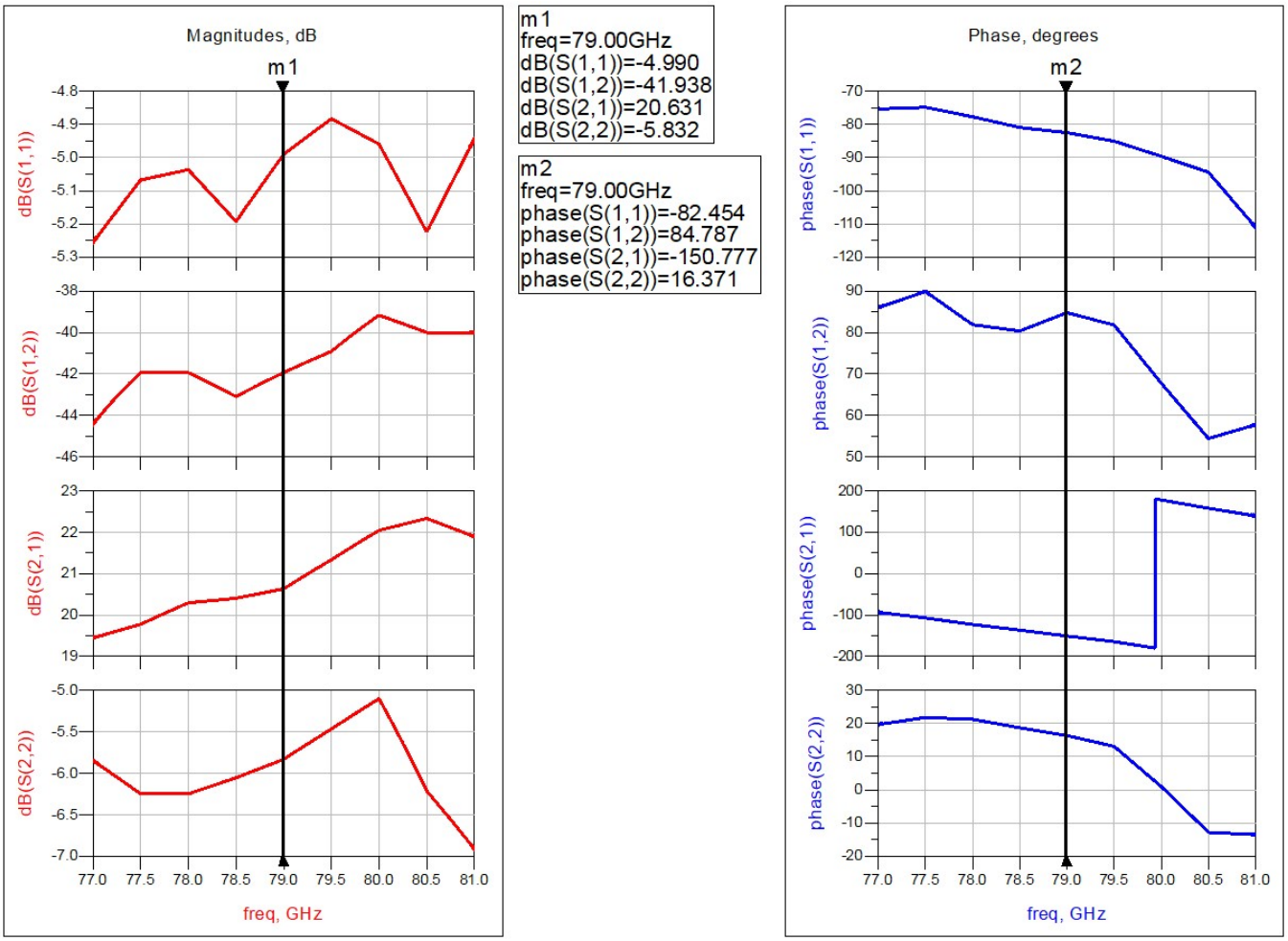

Figure 6: HMC-AUH320 S-Parameter Response

Observe that at the center, design frequency, the forward transmission, S_{21} gain parameter measures 20.631 dB. Additionally, the input return loss ($|S_{11}|$) measures approximately 5 dB at 79 GHz.

The results observed in Figure 6 concur with the results provided in the datasheet [3], verifying the operation of the amplifier.

5 Quadrature Couplers

The system block diagram shown in Figure 2 highlights several quadrature couplers. This section will provide a brief background for this component as well as the process taken to design an acceptable hybrid coupler at the 79 GHz center, design frequency.

5.1 Background

A hybrid coupler, often called a quadrature coupler, is a 3dB directional coupler with a 90° phase difference in the outputs of the through and coupled ports. A common type of quadrature coupler composed of microstrip lines is called a branch-line coupler. Each branch of the coupler is of electric length $\lambda/4$ with the top and bottom through branches having a characteristic impedance of $Z_o/\sqrt{2}$. Figure 7 highlights the above described geometry of the branch-line coupler that will be used for this design. Additionally, note that the second input, port 4 (of Figure 7) will be terminated and hence isolated.

$$[S] = \frac{-1}{\sqrt{2}} \begin{bmatrix} 0 & j & 1 & 0 \\ j & 0 & 0 & 1 \\ 1 & 0 & 0 & j \\ 0 & 1 & j & 0 \end{bmatrix} \tag{1}$$

Equation 1 represents the S-Matrix for a branch-line coupler. Evaluating this matrix, it is apparent that the outputs at ports 2 and 3 will both have half-power magnitudes, with -90 and -180 degree phase lags, respectively.

The output at port 2 (of Figure 7) can be evaluated by observing the S_{21} parameter. The phase component of this parameter is represented by a $-j$, which equates to $-\pi/2$ radians or $-90°$. The magnitude component of this parameter is $1/\sqrt{2}$, which yields a half-power, -3dB power loss.

The output at port 3 (of Figure 7) can be evaluated by observing the S_{31} parameter. The phase component of this parameter is represented by a -1, which equates to $-\pi$ radians or $-180°$. The magnitude component of this parameter is also $1/\sqrt{2}$, again yielding a half-power, -3dB power loss.

Since a $-180°$ phase lags ultimately simplifies to -1, this simply represents a signal inversion with a 0° phase lag, hence the outputs at port 2 and 3 are theoretically 90° out of phase, or in quadrature.

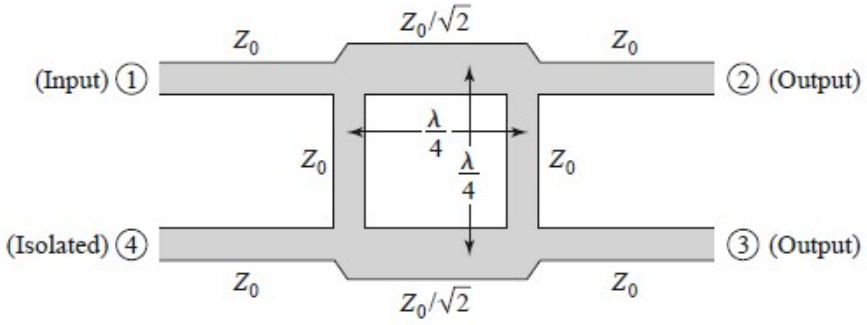

Figure 7: Geometry of a Branch-Line Quadrature Coupler [1]

5.2 Ideal Transmission Line Design

Following the theory described in Section 5.1 an ideal transmission line representation of the branch-line coupler can be designed to verify the design. Additionally, half-wave series lines were placed at each port to provide feed to the coupling geometry itself. Figure 8 below illustrates this ideal design.

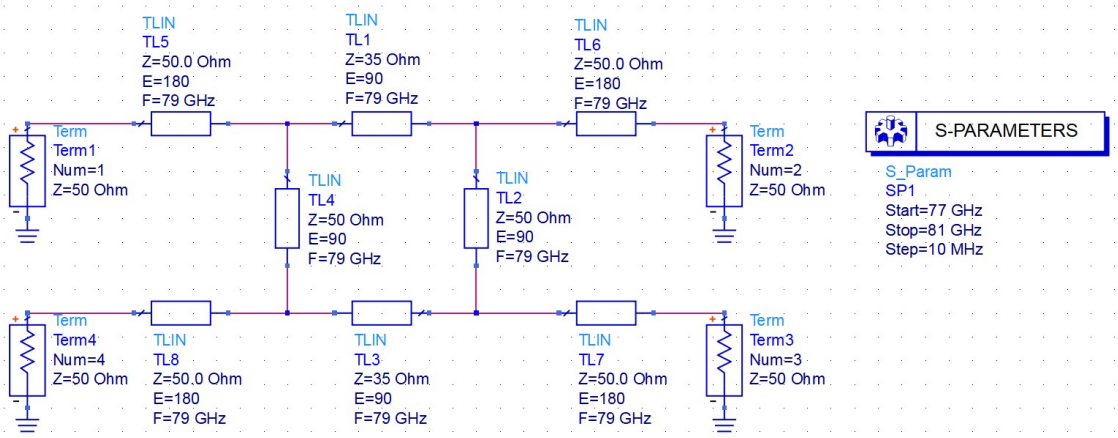

Figure 8: Branch-Line Coupler with ideal Transmission Lines

Figure 9 below highlights the S-Parameters results for the forward and coupled transmission with respect to input port 1 (S_{21} and S_{31}) and input port 4 (S_{34} and S_{24}). Note, the expected symmetries observed in the S-Parameters as well as the near perfect 3dB, half-power loss and 90° quadrature observed at the output ports 2 and 3, respectively.

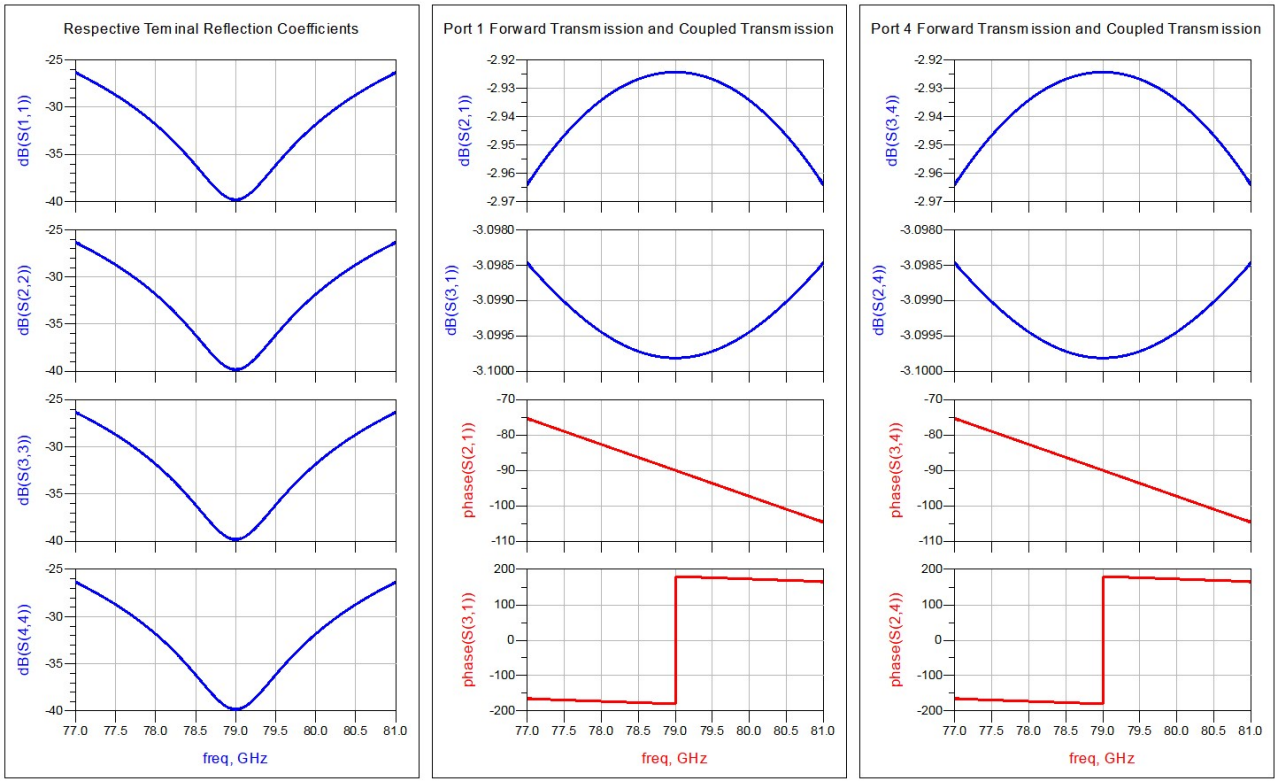

Figure 9: Branch-Line Coupler with Ideal Transmission Lines Simulation Results

5.3 Practical Microstrip Design

After the theoretical design was verified via the ideal transmission line model described in Section 5.2, a practical microstrip version of the design can be implemented.

First, an adequate substrate needs to be selected for the high frequency, millimeter wave application of this design. Rogers Corporation provides a variety of different substrate materials for high frequency applications, one of them being the RO3003 High Frequency Laminate material. This laminate has a specific application for automotive radar in the 77 GHz frequency band, which is perfect for this design. Table 3 below highlights the performance specifications for the RO3003 substrate.

Table 3: RO3003 Substrate Performance Specifications [4]

Parameter	Value	Unit
Dielectric Constant	3.00 ± 0.04	-
Dissipation Factor, tan δ	0.001	-
Standard Thickness, H	10	mils
Density	1.4	gm/cm^3
Standard Copper Thickness	0.5 / 17	oz / μm
Copper Conductivity (σ)	5.96e+7	S/m
Relative Permeability (μ_r)	1	-

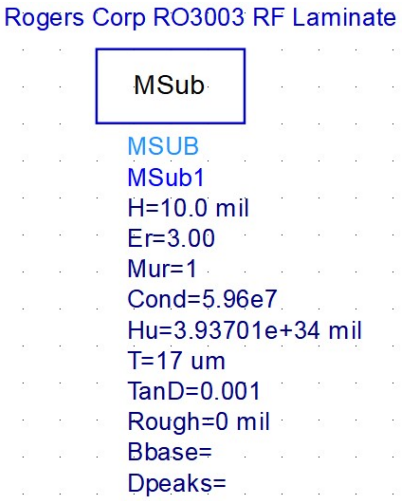

Figure 10: RO3003 Laminate Substrate Definition

Using the substrate definition noted in Figure 10, the Lincalc tool in ADS can be used to compute the physical lengths and widths of the microstrip lines to the corresponding design parameters of the ideal schematic shown in Figure 8. Table 4 below highlights the physical dimensions of the initial branch-line coupler design.

Table 4: Branch-line coupler initial physical dimensions

Electric Length (λ)	**Impedance** (Ω)	**Phase** ($^\circ$)	**Length (mils)**	**Width (mils)**
$\lambda/4$	50	90	23.14	27.2
$\lambda/4$	35	90	22.6	45.7
$\lambda/2$	50	180	46.3	27.2

Note, 50 Ω is the system characteristic impedance, Z_o, while 35 Ω is approximately $Z_o/\sqrt{2}$.

Figure 11 below highlights the initial branch-line design schematic, while Figure 12 illustrates its simulation results.

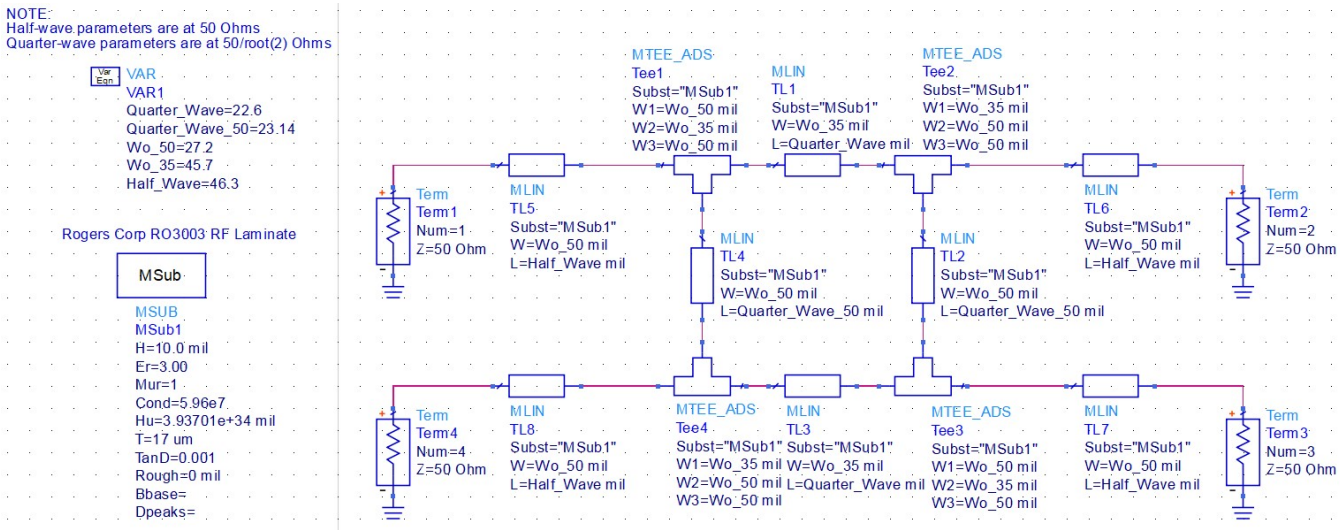

Figure 11: Initial Microstrip Branch-Line Coupler Design Schematic

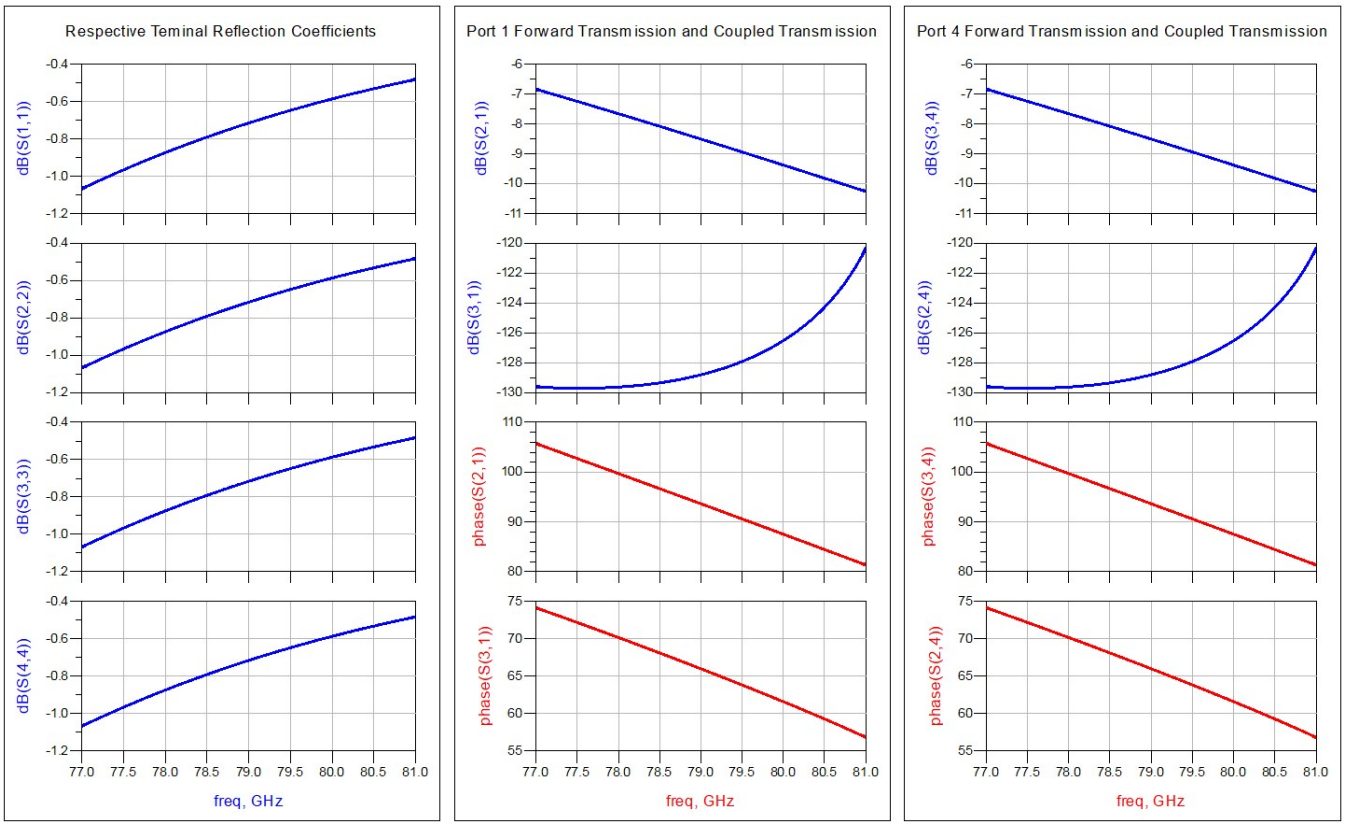

Figure 12: Initial Microstrip Branch-Line Coupler S-Parameter Results

Observe from Figure 12 that the initial simulation is far from what the expected results should be. Attenuation losses along with imprecision in physical dimensions at such high frequencies lead to losses over 10 dB at the center frequency with inconsistent phase relationships.

To alleviate these issues, optimization will be conducted on the design. Four goals were set:

1. Output port 2 magnitude greater than -3dB.
2. Output port 3 magnitude greater than -3dB.
3. Output port 2 phase within -100 to -80 degrees.
4. Output port 3 phase within -190 to -170 degrees.

Utilizing the *Hybrid* and *Quasi-Newton* Optimizers, the final results pictured in Figure 14 were achieved. Port 2 and 3 featured losses very near -3dB with astounding phase representations of -90 and -180 degrees at port 2 and 3, respectively. Figure 13 highlights the final branch-line coupler design schematic.

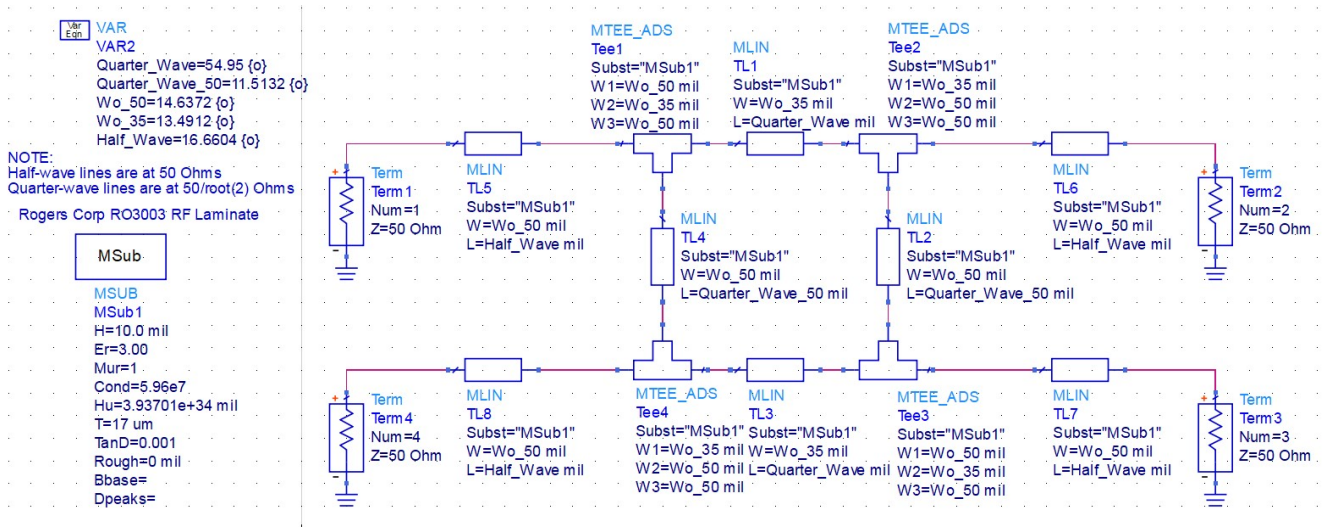

Figure 13: Final Microstrip Branch-Line Coupler Design Schematic

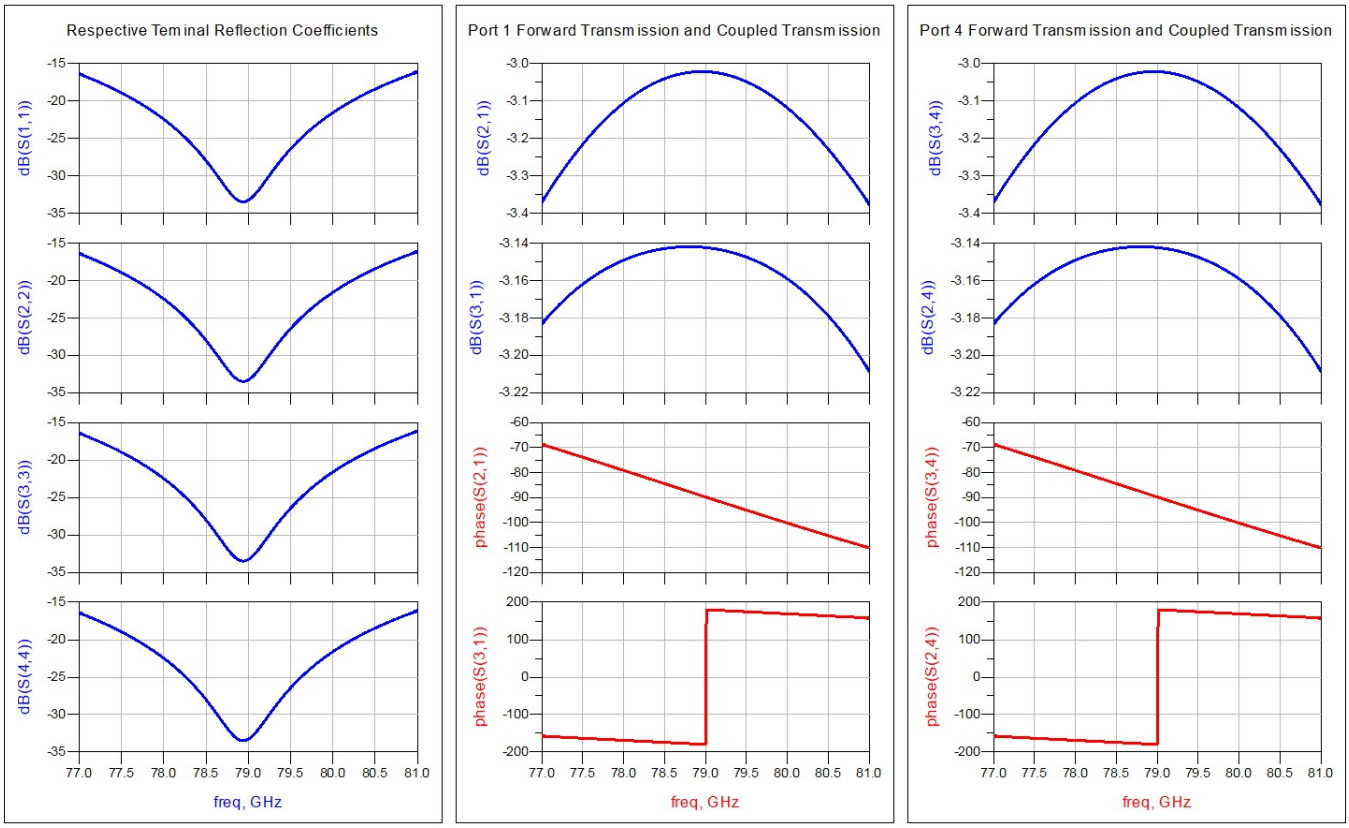

Figure 14: Final Microstrip Branch-Line Coupler S-Parameter Results

6 Butler Matrix

The input and output Butler Matrix pictured in the system block diagram are pivotal to the MPA design. They serve as the primary power combining components for this design. This section will discuss a brief background on Butler Matrices as well as the implemented design.

6.1 Background

In its simplest form, a Butler Matrix is a beam-forming network. They're most commonly found in phased-arrays and can be used to steer an antenna beam in a specific direction in one plane [8]. They utilize an array of 4 hybrid couplers, discussed in Section 5 with 45° phase lags between the top and bottom through paths, as observed in Figure 15.

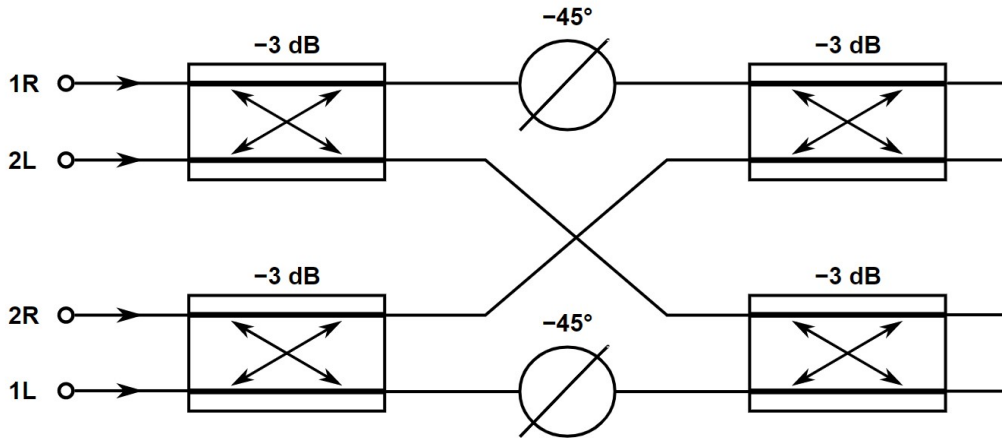

Figure 15: Geometry of a Butler Matrix (*reference 'Butler Matrix' via The Free Encyclopedia)*

Although beam forming is one feature of the Butler Matrix, the phase relationships characteristics of this network can be utilized to allocate and combine power to different antennas. The input Butler Matrix will split the power from the single input port to the four balanced amplifiers, while the output Butler Matrix combines and distributes the amplified power to the antennas. Since the hybrid coupler has already been designed in Section 5, the Butler Matrix can be constructed by simply utilizing four identical versions of this design along with additional intermediate microstrip lines used for phase shifting.

6.2 Design

To simplify the design and create clean schematics, multiple levels of symbols and sub-networks were created for the Butler matrix. To start off, the final branch-line coupler design from Figure 13 was placed in a separate schematic with it's replicate right below it. Pins were attached to each respective input and output port. This topology can be described as stacked couplers and is pictured in Figure 16. It was then placed into a symbol named Stacked_HybridCoupler, observed in Figure 17.

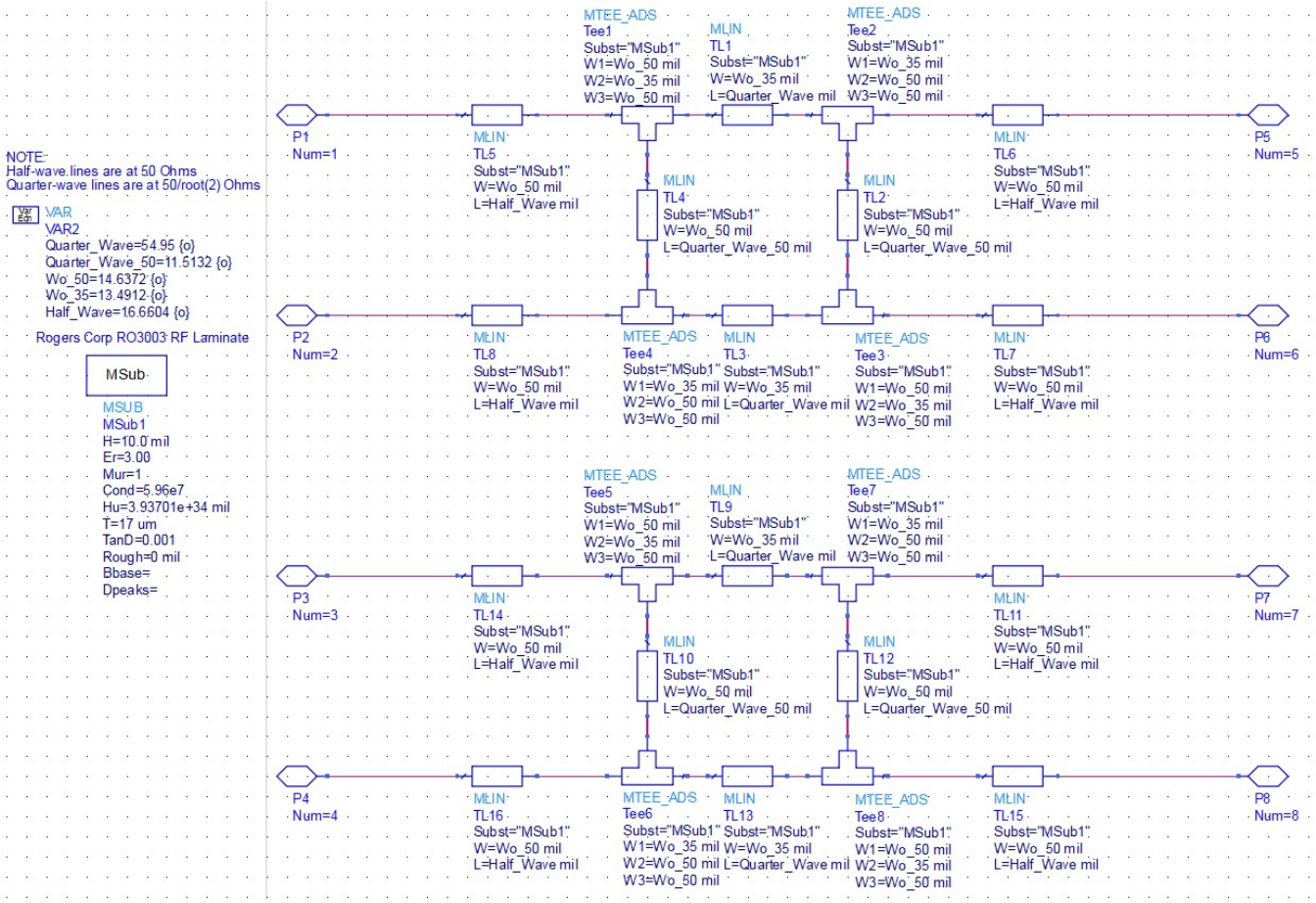

Figure 16: Stacked Couplers sub-network (internal) Schematic

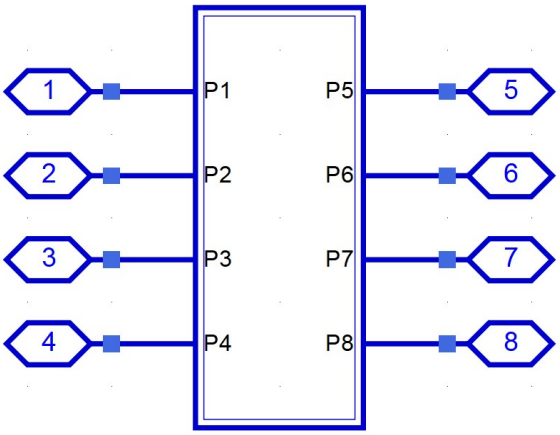

Figure 17: Stacked Couplers Symbol

This stacked coupler symbol can now be used with, again, a replicate of itself, to create the Butler Matrix shown in Figure 15. Figure 18 illustrates this topology. Note several aspects of this design:

- The intermediate eighth wave microstrip line serves as a 45° phase shifter for the top and bottom through paths.
- The second and third outputs of the first stacked coupler get switched to connect to the third and second inputs of the second stacked coupler, respectively. This is known as a crossover and for simulation purposes is just represented as flipping the wire lines.

Figure 19 represents the symbol created from the schematic described above and shown below in Figure 18.

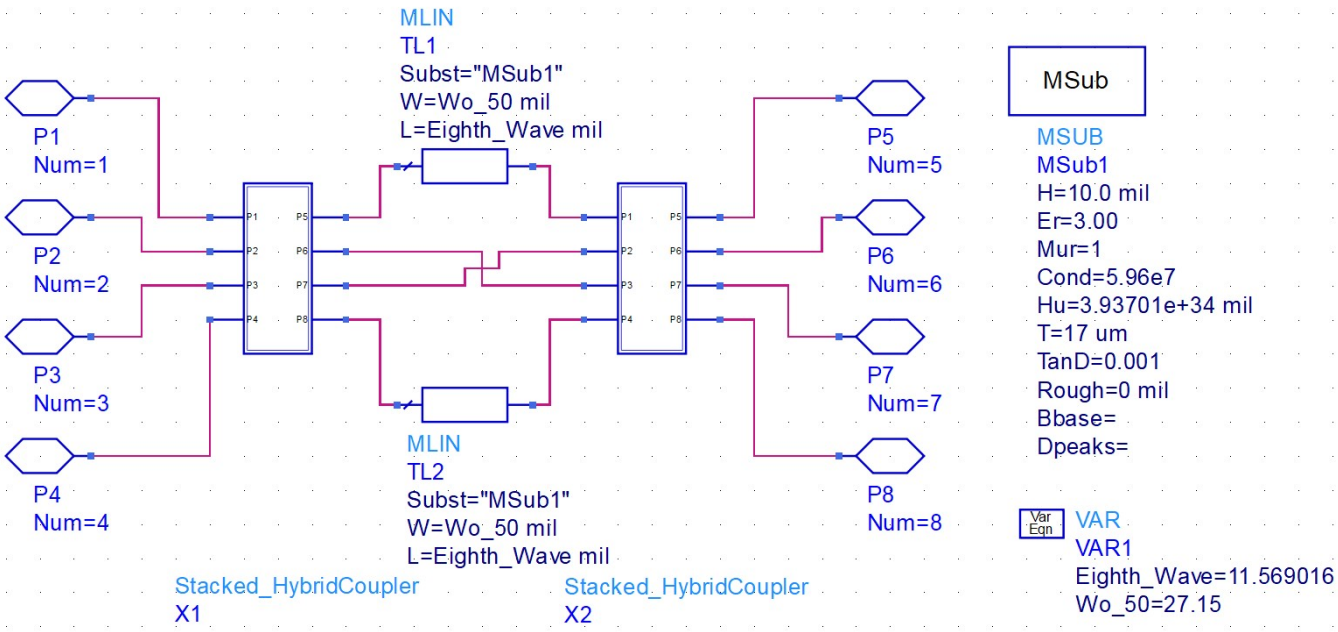

Figure 18: Butler Matrix sub-network (internal) Schematic

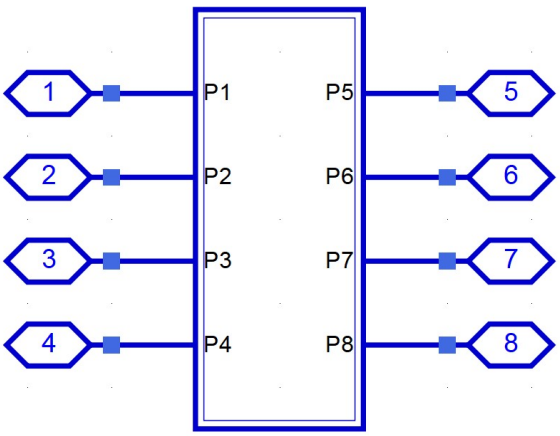

Figure 19: Butler Matrix Symbol

6.3 RF Performance

Now that the Butler Matrix has been designed, it's RF performance can be verified. Figure 20 below shows the schematic used to test and validate the Butler Matrix. A S-Parameter simulation was conducted on the component from 77 to 81 GHz.

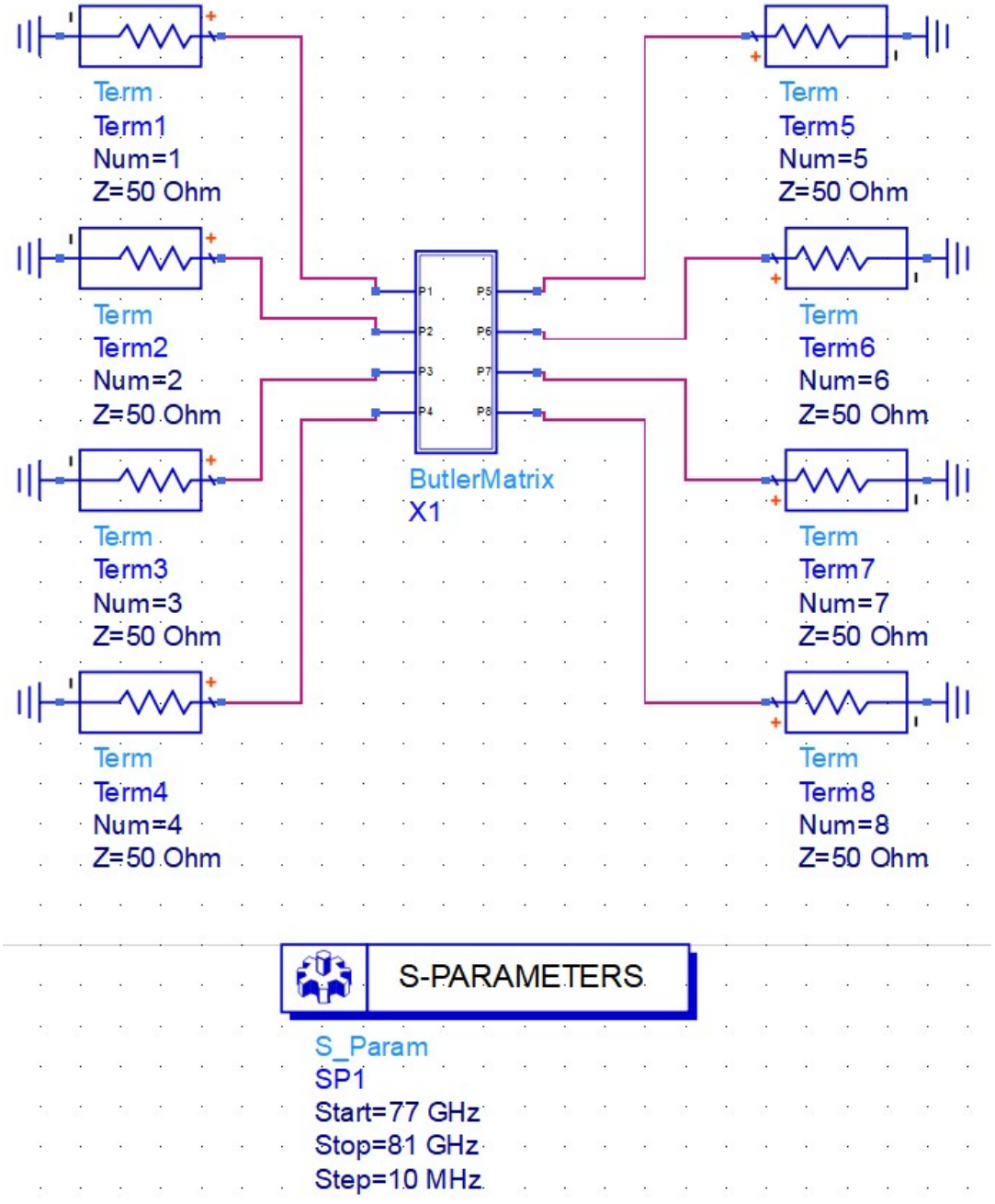

Figure 20: Butler Matrix Test Schematic

Figure 21 below highlights the S-Parameter simulation results. Observe the network performs strongly compared to the theoretical model, as summarized in Table 5.

Table 5: Theoretical vs. Simulated Butler Matrix results, input port 1 reference

S-Parameter	Theoretical	Simulated	% Difference (Mag. / Phase)
S_{51}	-6dB $\angle$ 135°	-6.056dB $\angle$ 135.353°	0.93 / 0.26
S_{61}	-6dB $\angle$ 45°	-6.178dB $\angle$ 45.253°	2.92 / 0.56
S_{71}	-6dB $\angle$ 90°	-6.162dB $\angle$ 90.336°	2.66 / 0.37
S_{81}	-6dB $\angle$ 0°	-6.281dB $\angle$ 0.097°	4.58 / NaN

Note, *only* input port 1 is analyzed since the three remaining input ports will be terminated. Reference Figure 20 for respective port numbering and locations.

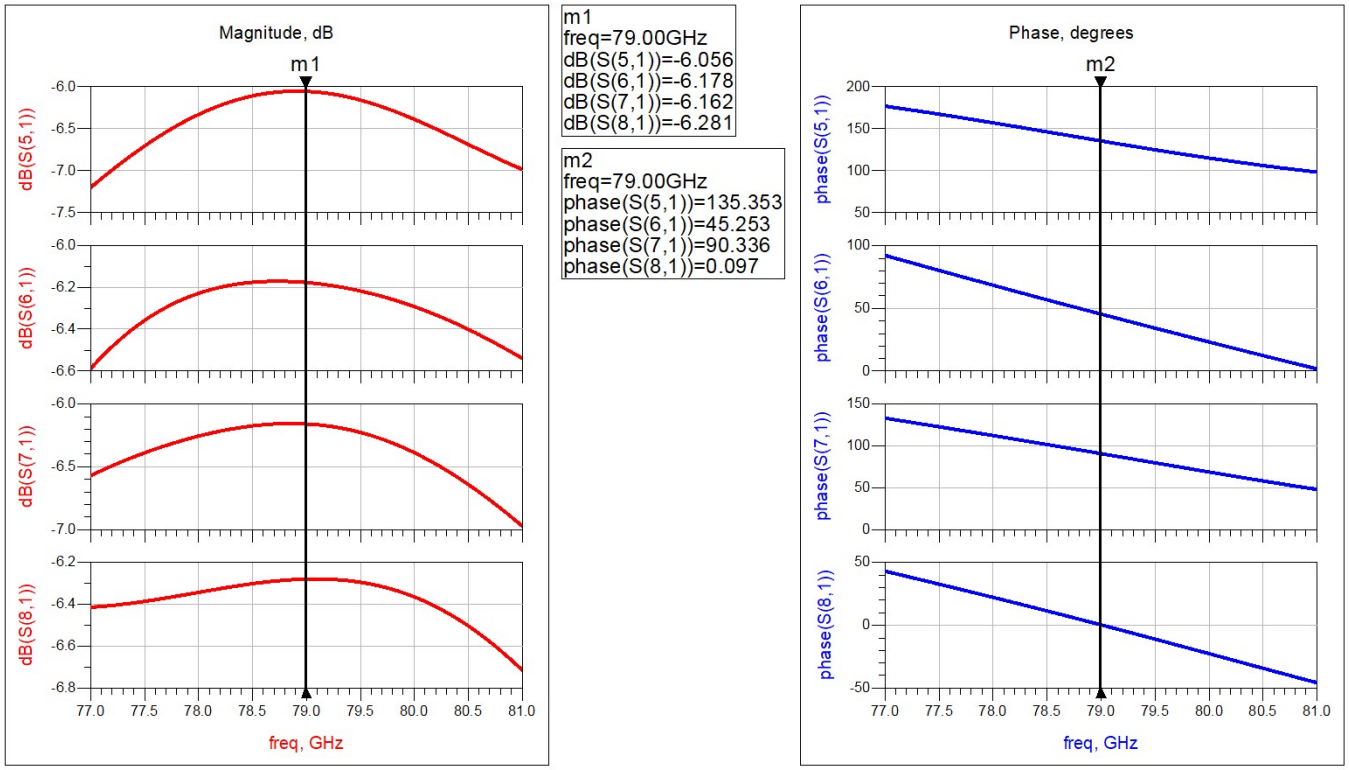

Figure 21: Butler Matrix S-Parameter Results

7 Phase Shifters and Matching Networks

Now that the Butler Matrix and Amplifiers have been designed, phase shifters and *necessary* Matching Networks can be implemented. This section will give a brief overview of the phase shifting topology chosen as well as a matching network designed.

7.1 Phase Shifters

Phase shifters serve as a pivotal component to the MPA. Without the addition of the phase shifters, power allocation of the outputs can not be dynamically controlled. For this design, one of the simplest forms of a phase shifter was used – a microstrip transmission line.

By adjusting the physical length of a transmission line, the electric length also becomes manipulated. As already seen, when electric length changes, the relative phase lag of the line also changes. Therefore, the transmission line physical lengths can be altered to directly adjust the phase shift of a signal propagating through the line. Section 9 will expand on this theory and highlight the relative phase shifts required to focus power at a single port or provide a balanced output power to all four ports.

Figure 22 below highlights the microstrip transmission lines used as phase shifters for this design. Length parameters L1 through L4 were all set as variables that could be directly controlled to adjust the corresponding phase. Wo represented each lines width, which varies the corresponding impedance of the line. This width parameter was also set as a variable to optimize in terms of power reflection and transmission.

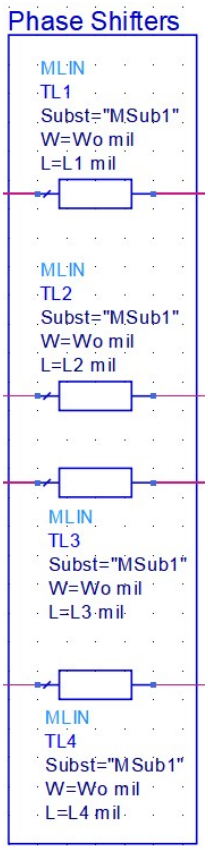

Figure 22: Phase Shifter Transmission Lines

7.2 Matching Networks

Matching Networks are a fundamental component of nearly every high frequency design. The purpose of a matching network is to matching two impedances in order to minimize reflections, hence maximizing transmission.

Although the system characteristic impedance is 50 Ω, the input/output impedance of several blocks have been adjusted in order to maximize power efficiency of the block. To ensure that this power efficiency is not corrupted when interconnecting components, special attention must be paid to components port impedances.

Through optimization, the input/output impedance of the Butler Matrix was shifted up to 65.2718 Ω. Being that the input Butler Matrix will be connected to the 50 Ω input terminals, an input matching network must be designed to match 50 Ω to 65.2718 Ω. The Butler Matrix output interconnection with the Phase Shifters can be ignored since the width (ultimately, impedance) of the Phase Shifters is a variable term to optimize power efficiency.

Similarly, the output Butler Matrix is interconnecting the Amplifiers to the Antennas. Given the amplifier has a matched output impedance of 50 Ω, a matching network needs to be assigned between the amplifier and output butler matrix in order to match 50 Ω to 65.2718 Ω. The output impedance of the butler matrix can again be ignored since it's being connected to a designed patch antenna, where the feed impedance will be specifically designed to match 65.2718 Ω.

There are several different Matching Network topologies, but a strong model that will be chosen for this high frequency design is a Double Stub tuner. This microstrip topology is favorable for wide-band matching and can be tuned utilizing shunt open-circuit stubs. Figure 23 illustrates the double stub tuner topology. Since both necessary matching networks described above need to match 50 Ω to 65.2718 Ω, a single design can be constructed.

To design this network, a MATLAB script was developed to compute the necessary electric lengths. A fixed $\lambda/8$ series stub will be used to interconnect the two shunt open-circuit stubs. Reference Appendix A for the MATLAB source code.

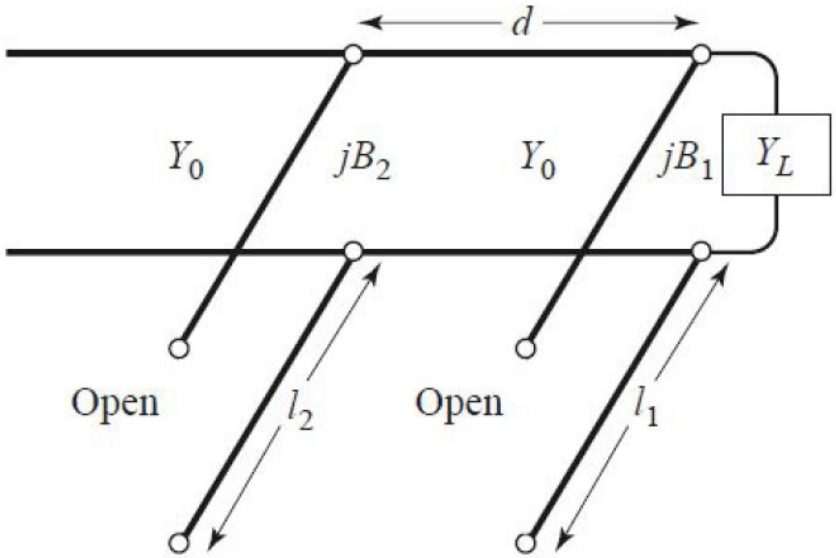

Figure 23: Double Stub Tuner Matching Network Diagram [1]

Table 6 below summarizes the design parameters that were attained via the MATLAB design script (reference Appendix A) and ADS's Lincalc tool.

Table 6: Matching Network Design Parameters via MATLAB script, reference Figure 24

Parameter	**Impedance (Ω)**	**Electric Length (λ / °)**	**Length (mils)**	**Width (mils)**
L_s	50	0.125 / 45	11.569016	27.154449
L_1	50	0.17531 / 63.1116	16.225315	27.154449
L_2	50	0.18394 / 66.2184	17.024055	27.154449

Figure 24 shows the final double stub tuner matching network design with a center, design frequency of 79 GHz.

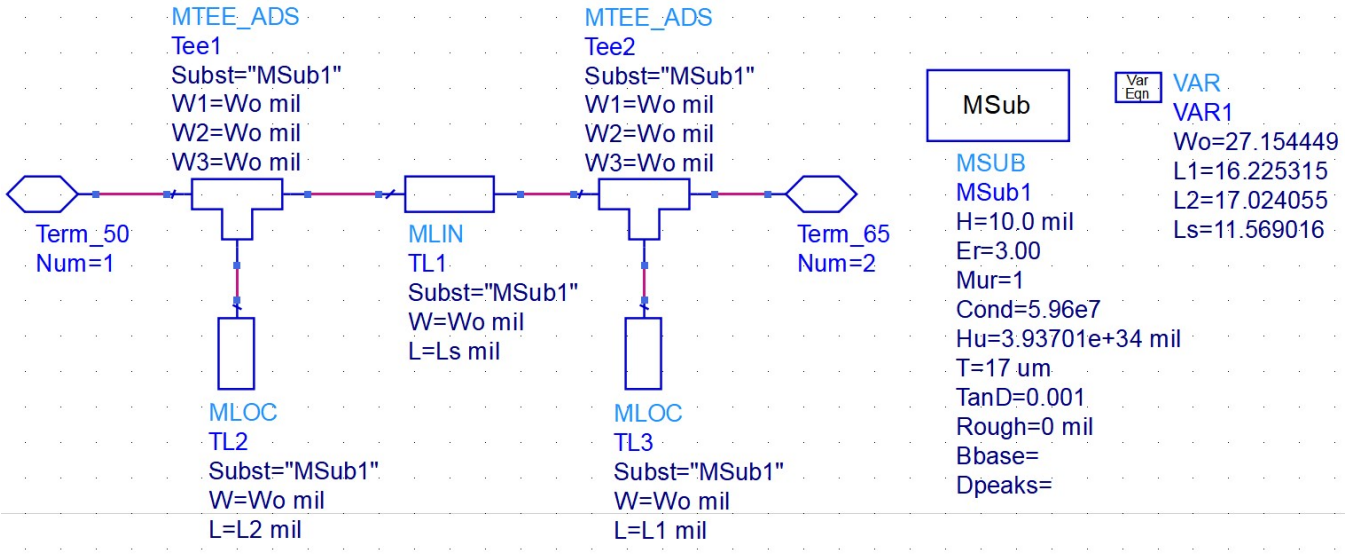

Figure 24: Matching Network sub-network (internal) Schematic

Figure 25 below represents the matching network symbol consisting of the internal, sub-network schematic shown above in Figure 24.

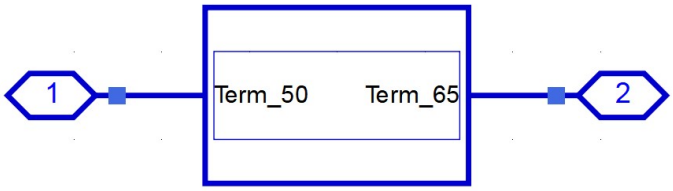

Figure 25: Matching Network Symbol

The designed matching network can now be tested to verify it's RF performance. Figure 26 represents a test schematic used to model an impedance translation of 50 Ω to 65.2718 Ω. An S-Parameter simulation was performed from 77 to 81 GHz.

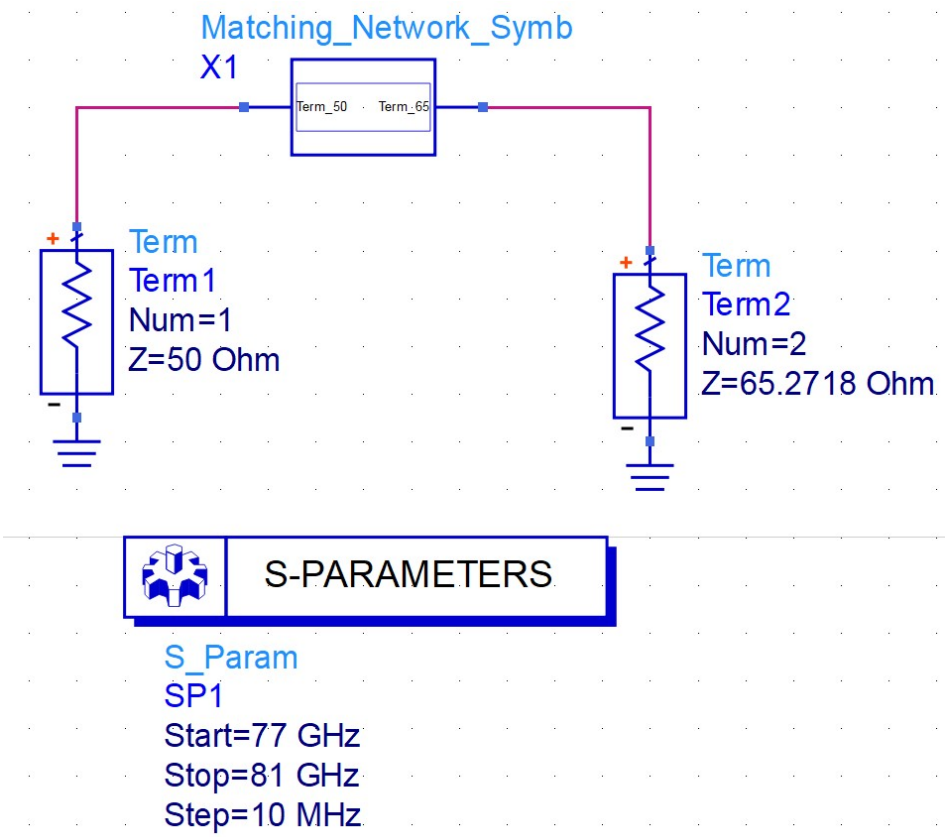

Figure 26: Matching Network Design Verification Test Schematic

Figure 27 below highlights the performance of the double-stub tuner matching network. The input reflection and forward transmission parameters are plotted versus frequency. The designed double-stub tuner boasts an exceptional -42.461 dB of input return loss and 0.070 dB of insertion loss at the center, design frequency of 79 GHz.

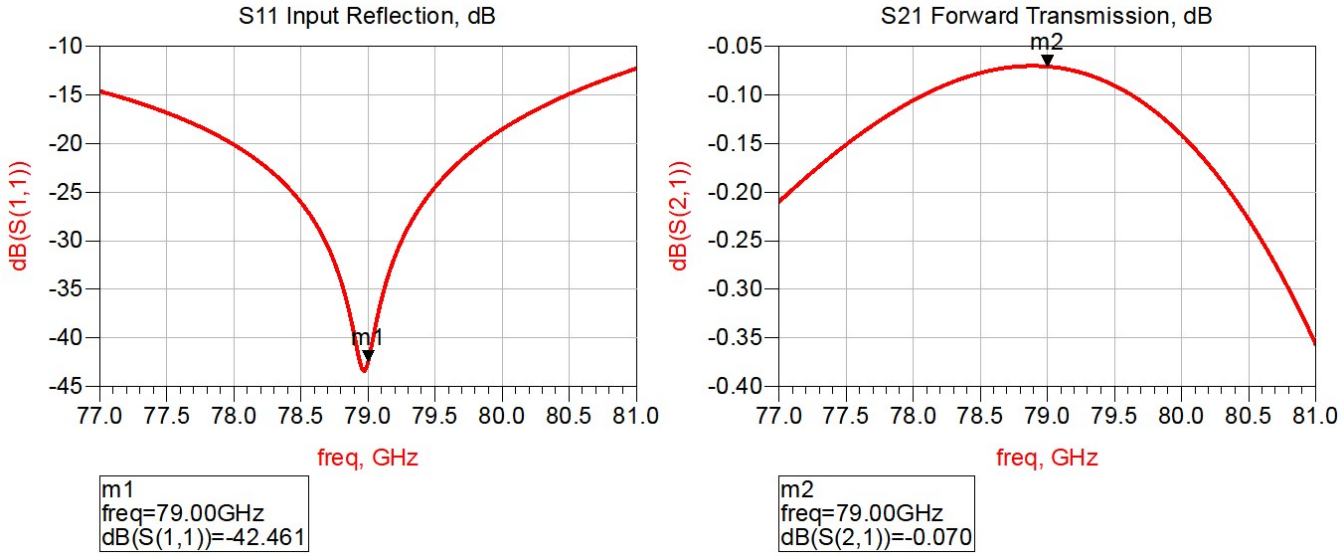

Figure 27: Matching Network Design Verification Simulation Results

8 Patch Antennas

The final component remaining in the system design is the Antenna. The antenna is again an important component to this design. It is also the most sensitive in terms of suffering from input return loss and power efficiency so special care must be taken during the design.

8.1 Antenna Type Selection

The first step in designing the antenna is selecting what type of antenna to use. A patch antenna was chosen for this design for several reasons. One being that it is feasible to design a patch antenna in Keysight ADS given it is simply conductive material geometrically printed on a substrate. Furthermore, the patch antenna is low-cost, low-profile, and can easily be fabricated [2]. Also, given the high frequency and resulting small physical dimensions of this design, a Patch Antenna can easily be integrated into the full system without sacrificing physical size.

8.2 Design and Layout

To design the antenna, the physical dimensions need to be computed based off of the design frequency and substrate parameters. The design frequency for this antenna will be the same 79 GHz center frequency. Additionally, the RO3003 substrate will again be used for this antenna design.

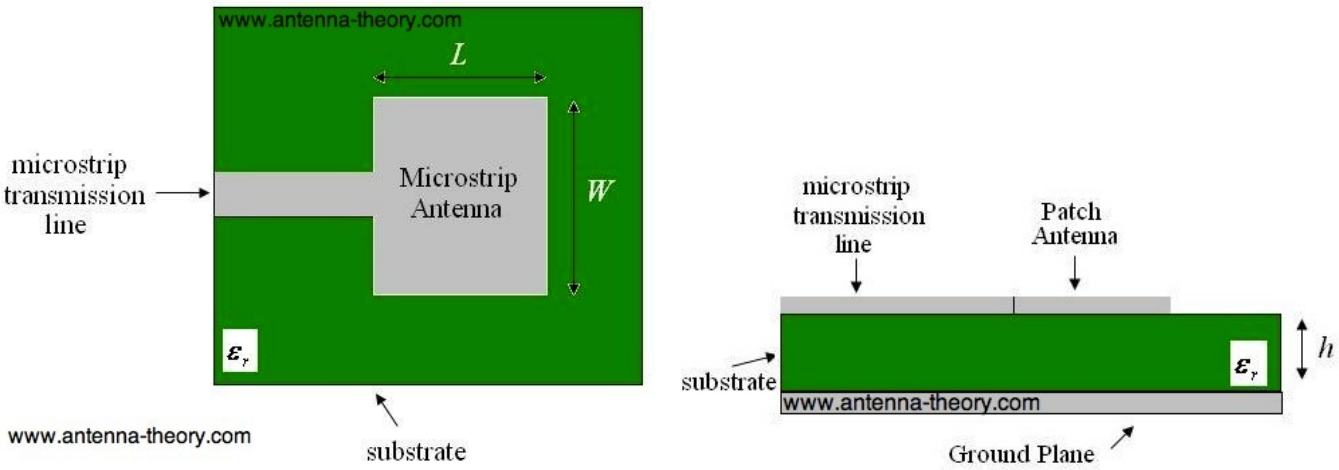

Figure 28: Geometry and Physical Parameters of a Patch Antenna [2]

$$W = \frac{c}{2f_o\sqrt{\frac{(\epsilon_r+1)}{2}}} \tag{2}$$

$$\epsilon_{eff} = \frac{\epsilon_r + 1}{2} + \frac{\epsilon_r - 1}{2}\left[1 + 12\frac{H}{W}\right]^{-1/2} \tag{3}$$

$$L_{eff} = \frac{c}{2f_o\sqrt{\epsilon_{eff}}} \tag{4}$$

$$\Delta L = 0.421H\frac{(\epsilon_{eff}+0.3)(\frac{W}{H}+0.264)}{(\epsilon_{eff}-0.258)(\frac{W}{H}+0.8)} \tag{5}$$

$$L = L_{eff} - 2\Delta L \tag{6}$$

Where,

f_o = resonance frequency = 79 GHz
W = Patch Width
L = Patch Length
H = Substrate thickness = 10 mils
ϵ_r = Substrate dielectric constant = 3.00
c = speed of light = 3.00×10^8

Note, all design equations above are referenced from [6] and [2].

Using the equations and definitions noted above, the patch antenna dimensions were attained.

An additional feature that will be added to the antenna design is a feed. This antenna feed will have a width that corresponds to the impedance of the output terminals of the output butler matrix (65.2718 Ω) in order to minimize reflections and maximize power transmission. The length will represent a $\lambda/4$ microstrip transmission line.

The full antenna design physical dimensions are summarized below in the Table 7.

Table 7: Patch Antenna Physical Dimensions

Parameter	**Value**	**Unit**
Patch Length, L	0.95108 / 37.44409449	mm / mils
Patch Width, W	1.34261 / 52.85866142	mm / mils
Feed Length	23.639606	mils
Feed Width	17.290394	mils

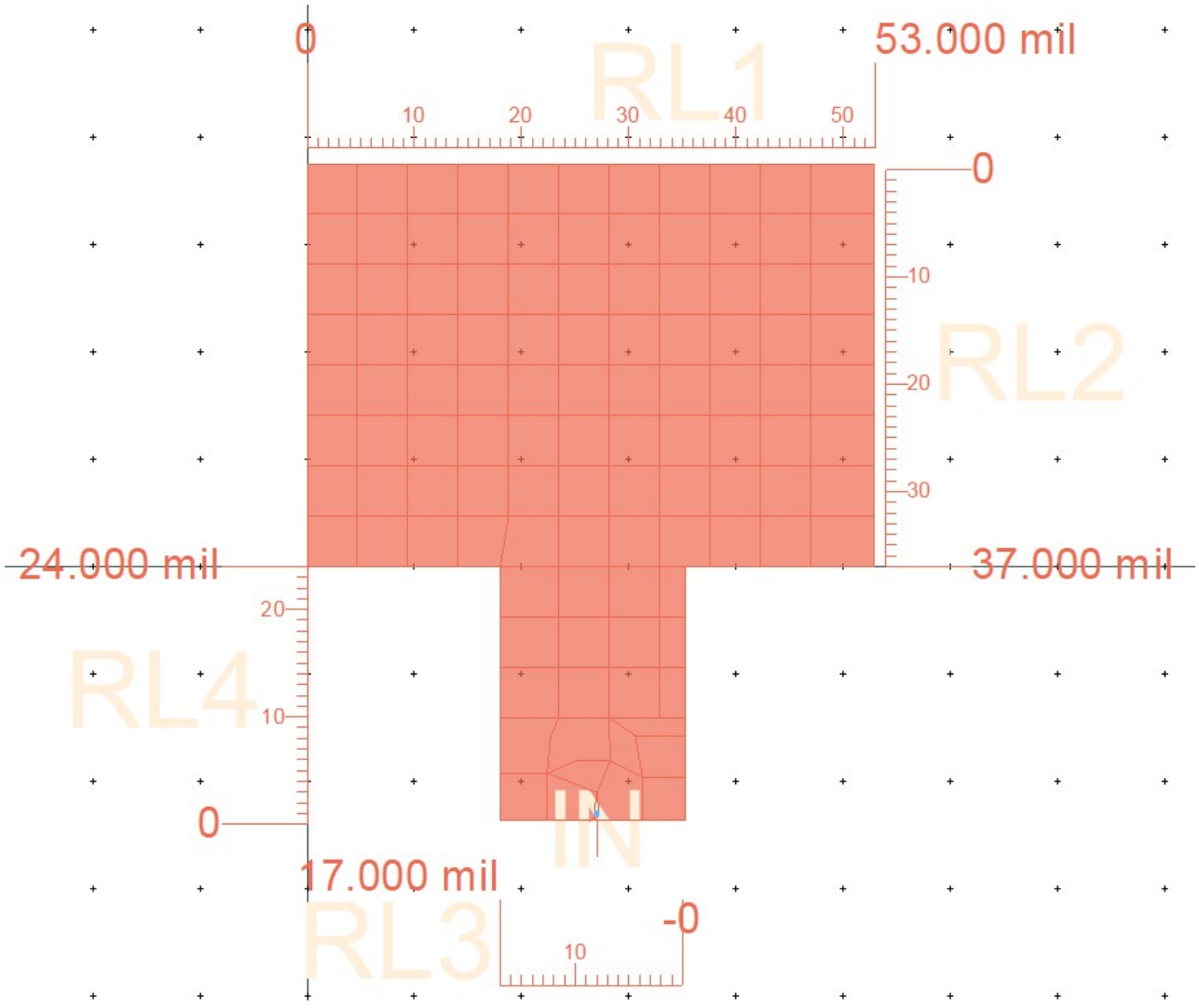

Figure 29: Patch Antenna Layout w/*Approximate* Dimensions

Figure 29 displays the Patch Antenna layout with approximate dimensions corresponding to those noted in Table 7.

In order to verify the antennas RF performance a substrate then had to be defined in ADS Momentum. Figure 30 illustrates the RO3003 defined substrate. It features a microstrip topology with a top open dielectric of air, copper conductor, RO3003 substrate, and a 0mil bottom perfect conductor (essentially just used as a bottom platform for simulation).

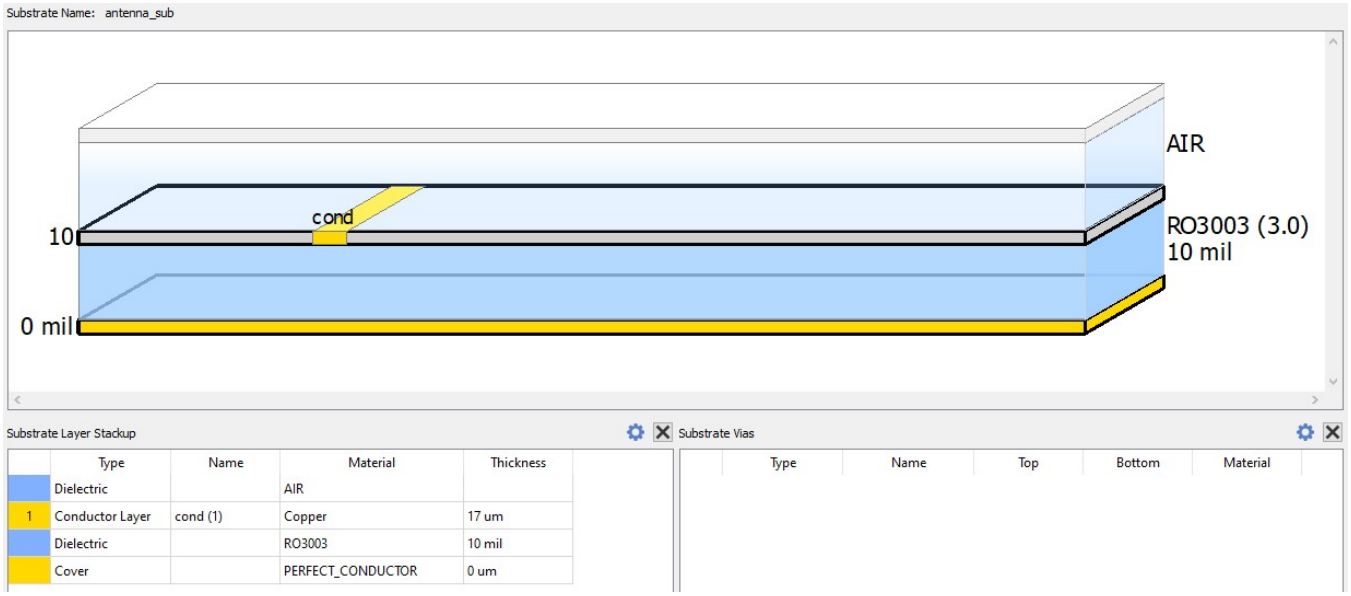

Figure 30: Momentum RO3003 Substrate Definition

Now that the antenna has been designed and a substrate has been defined, the RF performance can be verified.

8.3 Antenna Performance

Keysight Momentum is a 3D planar electromagnetic (EM) simulator that enables RF and microwave designers to simulate and optimize their designs [9]. It utilizes Method of Moments (MoM) technology along with microwave full-wave simulations to compute EM solvers and model real layout characteristics such as parasitics, coupling, the skin effect, and the substrate effect.

Momentum was utilized to characterize the antenna design discussed in Section 8.2. Figure 31 summarizes the simulated Antenna parameters for this design at the resonance frequency of 79 GHz. Note a favorable directivity of approximately 8 dBi, but a low antenna gain of approximately 3.2 dB and a radiation (power) efficiency of approximately 33% or $\approx -4.8\ dB$. Also, note the angle of max radiation intensity being $(\theta, \phi) = (29°, 90°)$. This points 29 degrees downward in the YZ-plane relative to a $+\hat{Z}$-orthogonal vector referenced from the X-plane.

Antenna Parameters

Frequency (GHz)		79
Input power (Watts)		0.00240184
Radiated power (Watts)		0.000791469
Directivity(dBi)		8.02805
Gain (dBi)		3.20695
Radiation efficiency (%)		32.9526
Maximum intensity (Watts/Steradian)		0.000399972
Effective angle (Steradians)		1.97881
Angle of U Max (theta, phi)	29	90
E(theta) max (mag,phase)	0.548962	13.9563
E(phi) max (mag,phase)	0.00195791	-0.69193
E(x) max (mag,phase)	0.00195791	179.308
E(y) max (mag,phase)	0.480133	13.9563
E(z) max (mag,phase)	0.266142	-166.044

Figure 31: Momentum Simulated Antenna Parameters at 79 GHz

Figure 32 below highlights the input return loss of the antenna. The target, acceptable value of -10 dB was just surpassed, with the antenna featuring a $S_{11} = -10.314dB \angle -156.584°$ at 79GHz. This yields 9.3% of the signal being reflected at the input of the antenna.

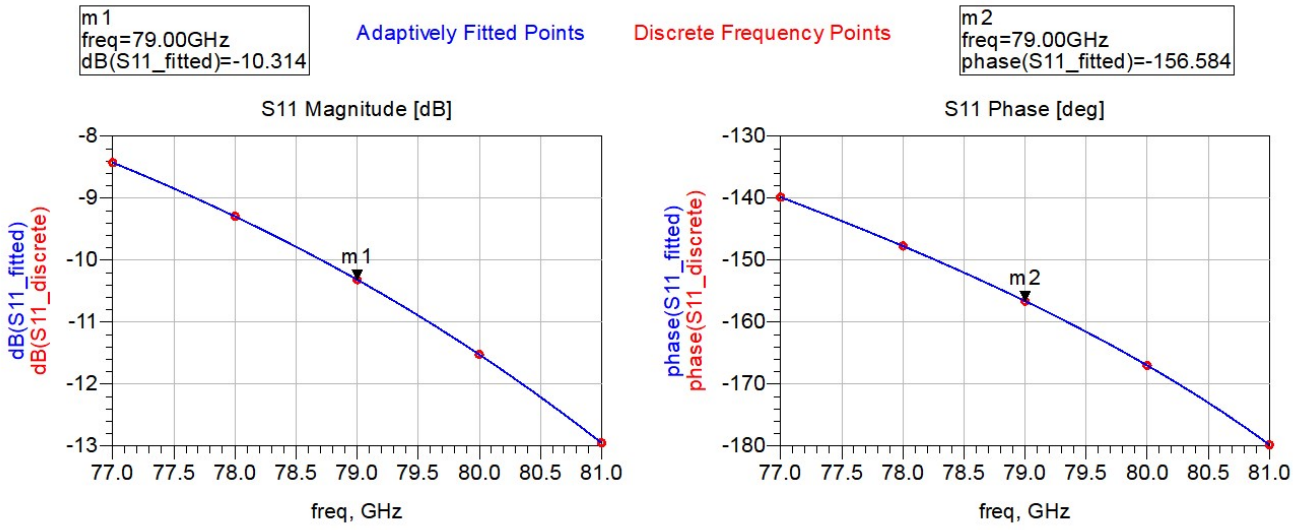

Figure 32: Momentum Simulation Input Reflection, S_{11}

Figure 33 below displays the antenna gain and directivity at two fixed ϕ angles, while sweeping θ.

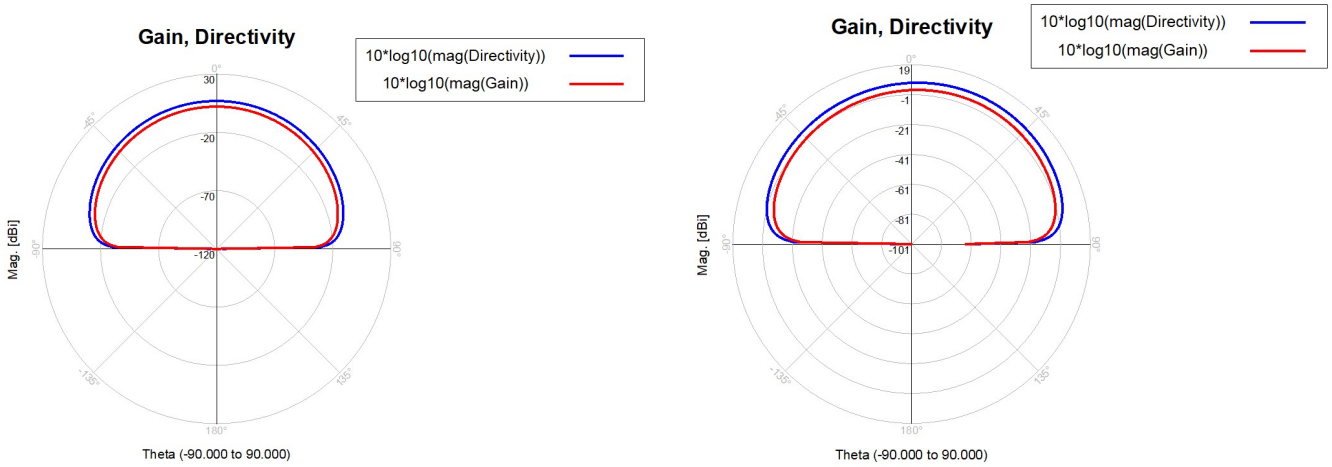

(a) $\phi = 0°$ (b) $\phi = 90°$

Figure 33: Antenna Gain and Directivity Plots for $\theta[-90°, +90°]$

Figure 34 below displays the antenna radiation intensity at two fixed ϕ angles, while sweeping θ.

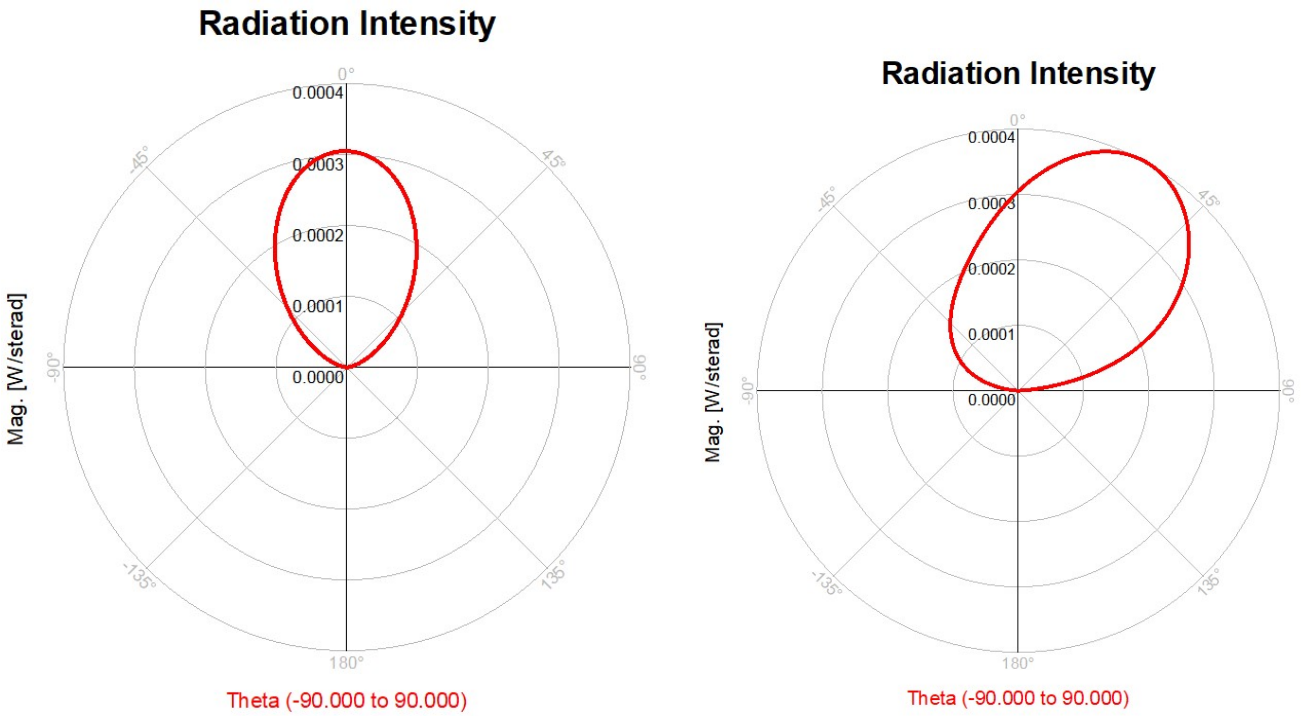

(a) $\phi = 0°$ (b) $\phi = 90°$

Figure 34: Antenna Radiation Intensity Plots for $\theta[-90°, +90°]$

Additionally, Figure 35 represents a 3D model of the far-field antenna (E-field) radiation pattern at 79 GHz. It shows how the antenna radiates in all directions bounded from $\phi[0°, 360°]$ and $\theta[-90°, +90°]$

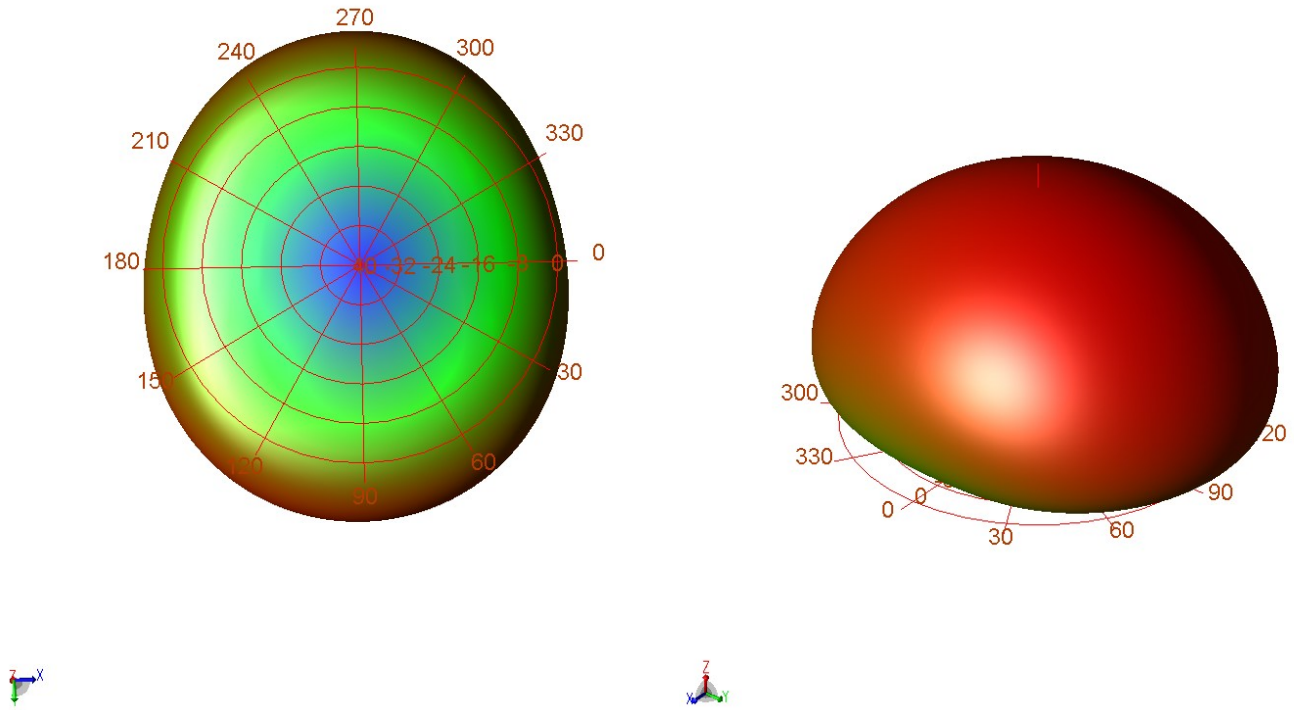

(a) Display 1 (b) Display 2

Figure 35: Antenna Far-field Radiation Pattern, Cartesian Coordinate System with ϕ Angle Annotations

Figure 36 represents a 3D model of the far-field current density at 79 GHz. This simulation demonstrates how the skin effect plays a role on this antenna design.

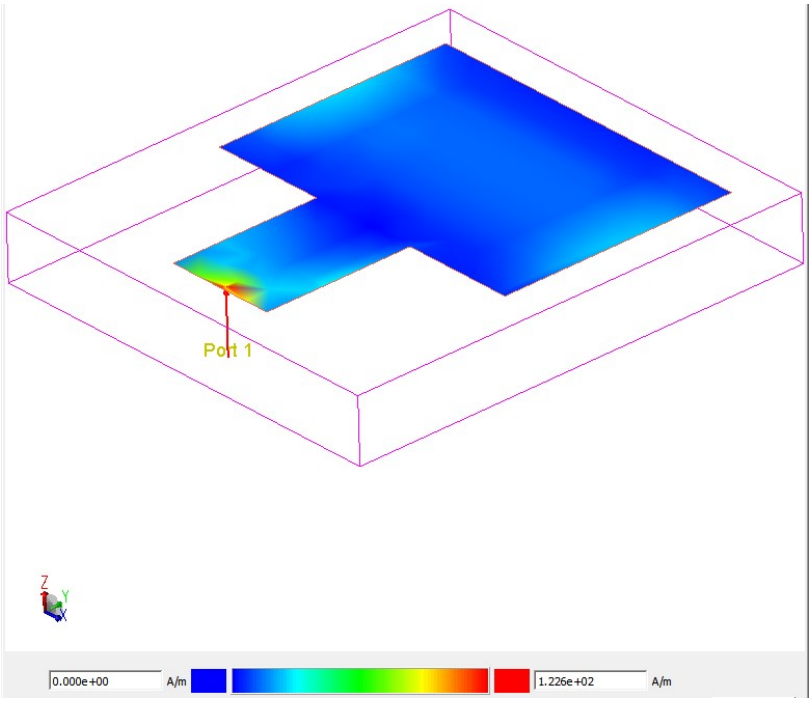

Figure 36: Antenna Far-field Current Density (A/m)

9 System Testing

With a full design, system level testing can now be performed. The main objective of this system level testing is to see how phase shifting can either focus and maximize full system power to a single output port, or distribute power equally among all four output ports.

9.1 Full System Design

Figure 37 highlights the full MPA and Antenna System design. For this section, output terminals will be referred to as OUTn, where n is the port number 1 through 4. Output port 1 is top output port, followed by 2, 3, and 4 descending downward. Figure 37 illustrates this relationship.

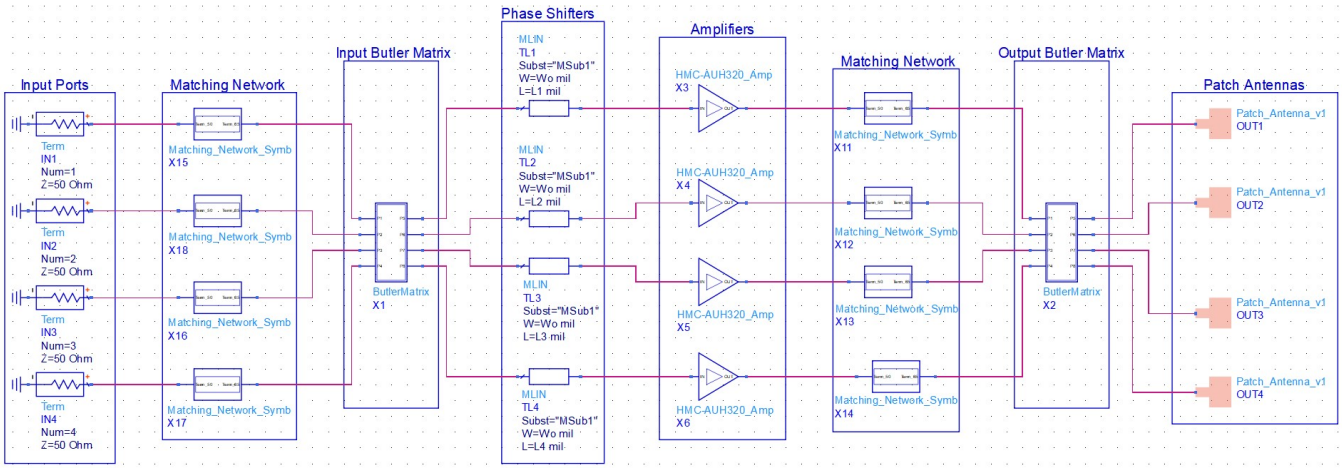

Figure 37: Full System Schematic

Figure 38 below illustrates the full system design gain budget for a single path. Observe from this figure that a full system gain of approximately 7.84dB can be achieved, excluding the antenna. Including the antenna, a gain of 11.84dB can be attained. Note, the figure states these values in terms of output power assuming an input of 0dB – this is equivalent to the gain parameter.

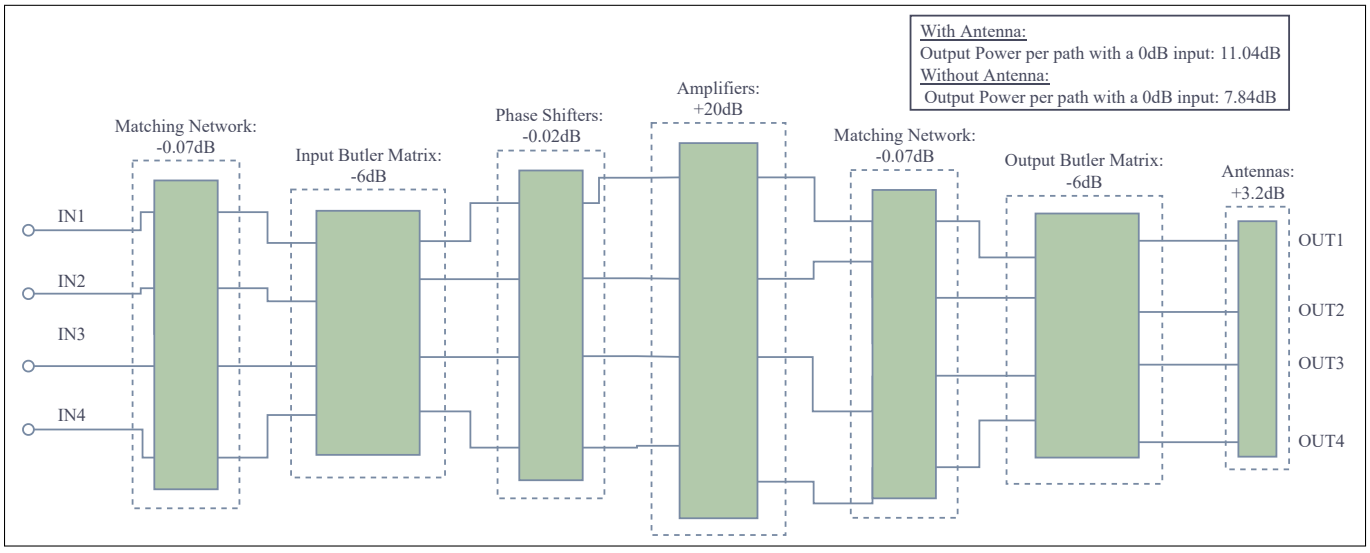

Figure 38: System Gain Budget

Note, all testing will be performed only utilizing a single input, IN1, with the remaining being matched terminated.

9.2 OUT1 Port Single Output

The first test and optimization process that was performed was to maximize power at the OUT1 output port. To accomplish this, the width and lengths of the four phase shifters discussed in Section 7.1 were varied. By varying the lengths, the associated phase of each path was proportionally varied. Adjusting the phases of each path can allow for power combination at a single port, which was the goal.

To find the appropriate phases to maximize power at the first output port, OUT1, the *Quasi-Newton* and *Hybrid* optimizers were used to adjust the four length variables, L1 through L4 and their associated widths, Wo.

Figure 39 shows the resulting physical dimensions that were found to attain a maximized gain of 20.04 dB at the center, design frequency of 79 GHz.

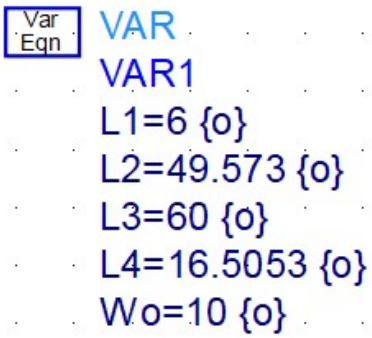

Figure 39: Single OUT1 Port Focused Power Phase Shifter Values

Table 8: Final Variable Parameters to Maximize Power at Output Port OUT1

Parameter	Physical Dimension (mils)	Electrical Property	Value	Unit
$L1$	6	Phase Shift	22.2791	°
$L2$	49.573	Phase Shift	184.0740	°
$L3$	60	Phase Shift	222.7910	°
$L4$	16.5053	Phase Shift	61.2872	°
Wo	10	Line Impedance	86.5178	Ω

Figure 40 below illustrates the S-Parameter forward gain results for each respective output port. Note, the top first plot represents the forward transmission observed at port OUT1 with respect to port IN1.

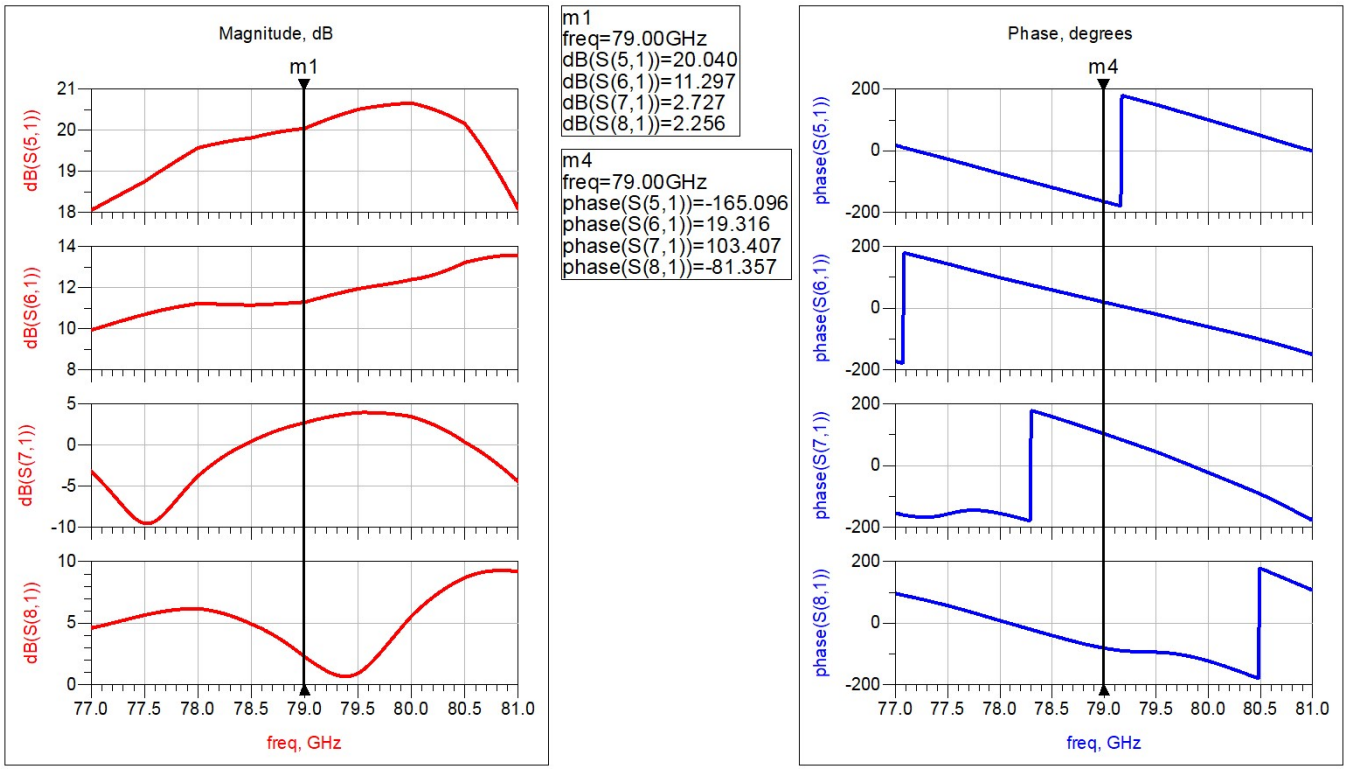

Figure 40: Single OUT1 Port Focused Power Simulation Results

9.3 OUT2 Port Single Output

The second test and optimization process that was performed was to maximize power at the OUT2 output port. To accomplish this, the same optimization process was performed.

Figure 41 shows the resulting physical dimensions that were found to attain a maximized gain of 19.9 dB at the center, design frequency of 79 GHz.

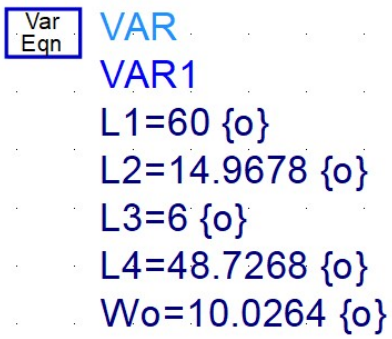

Figure 41: Single OUT2 Port Focused Power Phase Shifter Values

Table 9: Final Variable Parameters to Maximize Power at Output Port OUT2

Parameter	Physical Dimension (mils)	Electrical Property	Value	Unit
$L1$	60	Phase Shift	222.8160	°
$L2$	14.9678	Phase Shift	55.5845	°
$L3$	6	Phase Shift	22.2816	°
$L4$	48.7268	Phase Shift	180.9520	°
Wo	10.0264	Line Impedance	86.4126	Ω

Figure 42 below illustrates the S-Parameter forward gain results for each respective output port. Note, the second plot represents the forward transmission observed at port OUT2 with respect to port IN1.

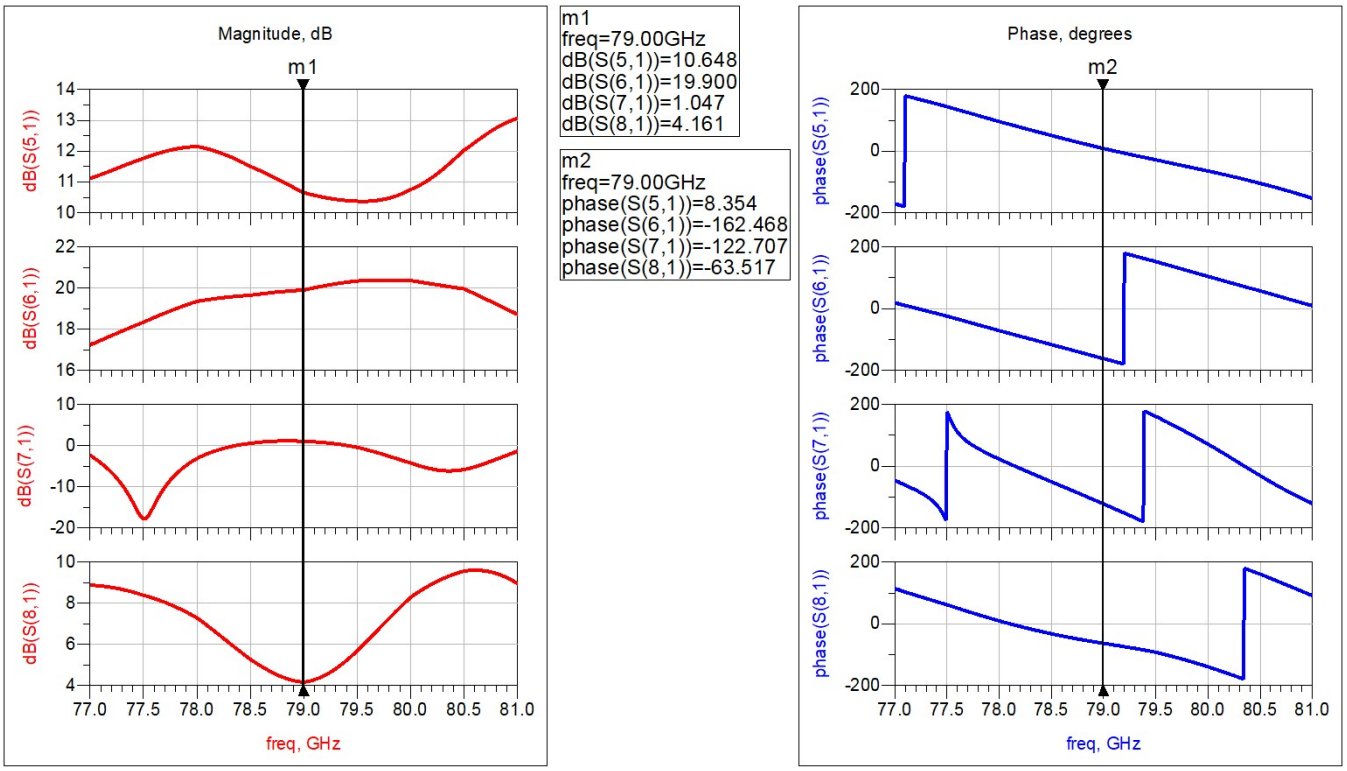

Figure 42: Single OUT2 Port Focused Power Simulation Results

9.4 OUT3 Port Single Output

The third test and optimization process that was performed was to maximize power at the OUT3 output port. To accomplish this, again, the same optimization process was performed.

Figure 43 shows the resulting physical dimensions that were found to attain a maximized gain of 20.993 dB at the center, design frequency of 79 GHz.

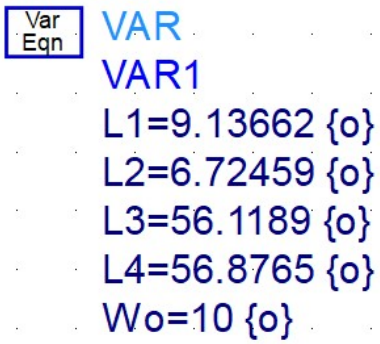

Figure 43: Single OUT3 Port Focused Power Phase Shifter Values

Table 10: Final Variable Parameters to Maximize Power at Output Port OUT3

Parameter	**Physical Dimension (mils)**	**Electrical Property**	**Value**	**Unit**
$L1$	9.13662	Phase Shift	33.9259	°
$L2$	6.72459	Phase Shift	24.9696	°
$L3$	56.1189	Phase Shift	208.3800	°
$L4$	56.8765	Phase Shift	211.1930	°
Wo	10	Line Impedance	86.5178	Ω

Figure 44 below illustrates the S-Parameter forward gain results for each respective output port. Note, the third plot represents the forward transmission observed at port OUT3 with respect to port IN1.

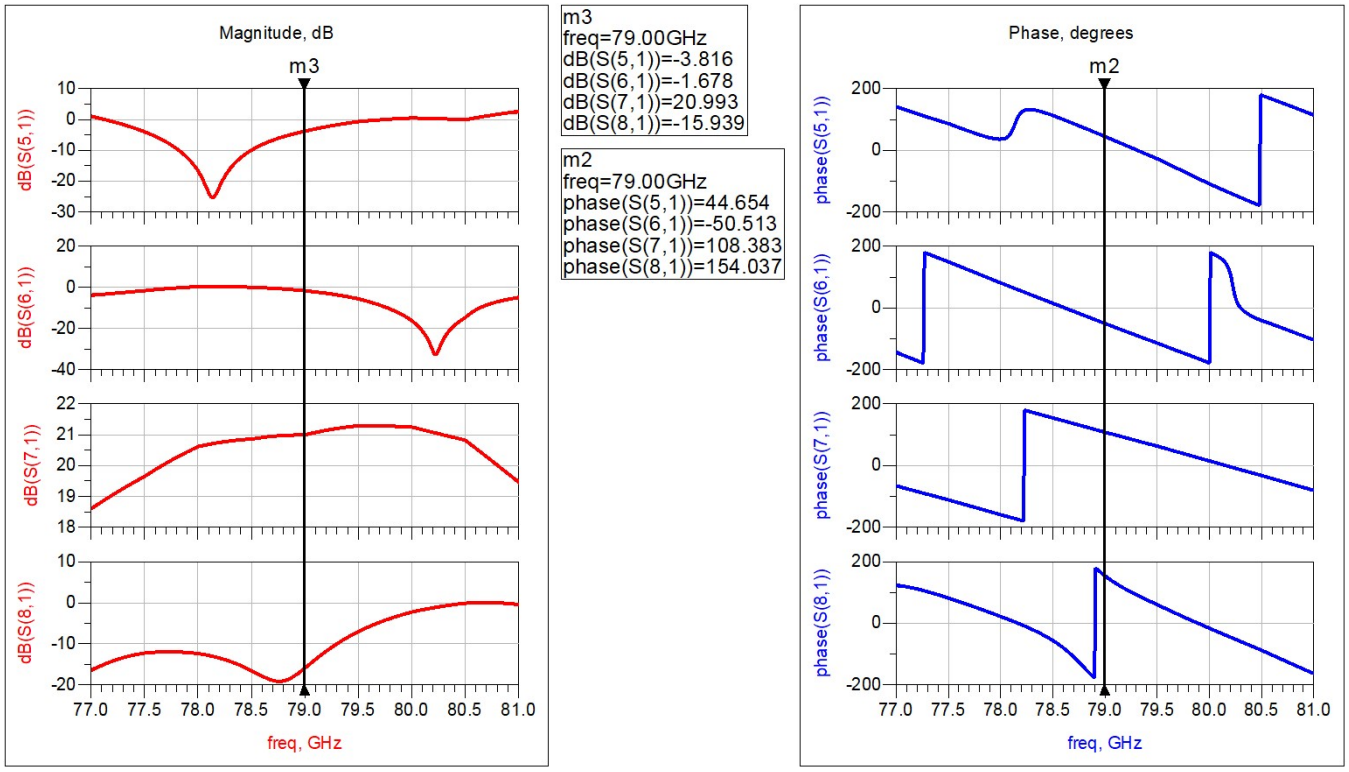

Figure 44: Single OUT3 Port Focused Power Simulation Results

9.5 OUT4 Port Single Output

The final focused power test and optimization process that was performed was to maximize power at the OUT4 output port. To accomplish this, the same optimization process was performed as the previous three cases.

Figure 45 shows the resulting physical dimensions that were found to attain a maximized gain of 20.996 dB at the center, design frequency of 79 GHz.

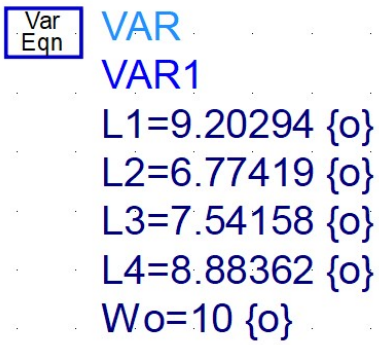

Figure 45: Single OUT4 Port Focused Power Phase Shifter Values

Table 11: Final Variable Parameters to Maximize Power at Output Port OUT4

Parameter	Physical Dimension (mils)	Electrical Property	Value	Unit
$L1$	9.20294	Phase Shift	34.1722	°
$L2$	6.77419	Phase Shift	25.1538	°
$L3$	7.54158	Phase Shift	28.0033	°
$L4$	8.88362	Phase Shift	32.9865	°
Wo	10	Line Impedance	86.5178	Ω

Figure 46 below illustrates the S-Parameter forward gain results for each respective output port. Note, the fourth bottom plot represents the forward transmission observed at port OUT4 with respect to port IN1.

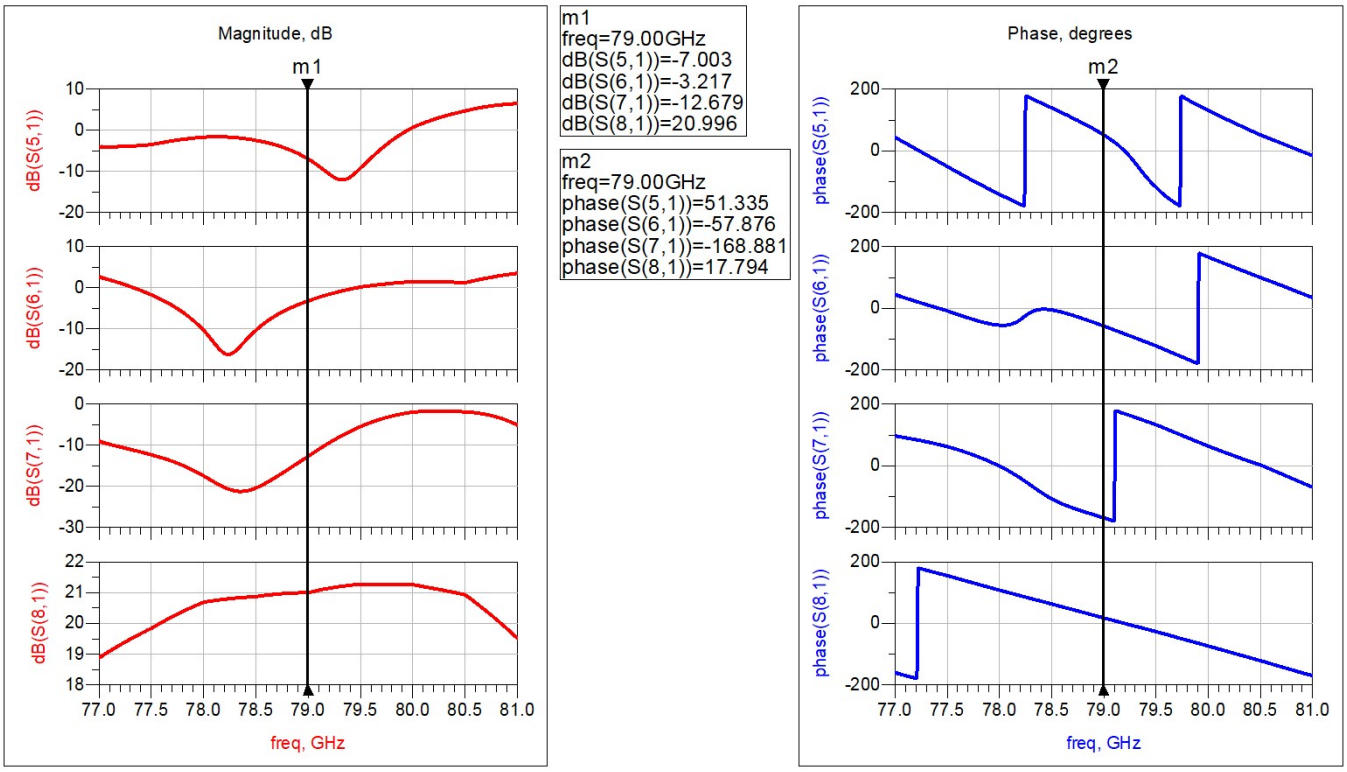

Figure 46: Single OUT4 Port Focused Power Simulation Results

9.6 Balanced Four Port Output

The overall final system level test and optimization process that was performed was to achieve a maximized, *balanced* output power at *all* four output ports To accomplish this, a similar optimization process was performed to vary L1 through L4 and Wo in order to satisfy specific gain requirements at *all four output ports*.

Figure 47 shows the resulting physical dimensions that were found to attain a maximized, balanced gain of approximately 15 dB at all four output ports at the center, design frequency of 79 GHz.

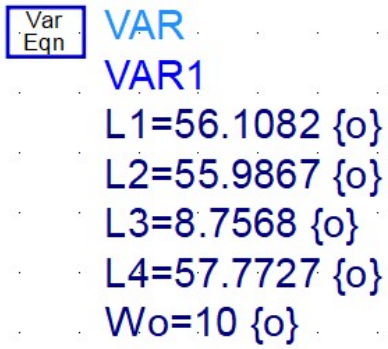

Figure 47: Balanced Four Port Power Phase Shifter Values

Table 12: Final Variable Parameters to Balance and Maximize Power at *all* Output Ports

Parameter	**Physical Dimension (mils)**	**Electrical Property**	**Value**	**Unit**
$L1$	56.1082	Phase Shift	208.3400	°
$L2$	55.9867	Phase Shift	207.8890	°
$L3$	8.7568	Phase Shift	32.5156	°
$L4$	57.7727	Phase Shift	214.5210	°
Wo	10	Line Impedance	86.5178	Ω

Figure 48 below illustrates the S-Parameter forward gain results for each respective output port. Note, all four plots represents the forward transmission observed at ports OUT1, OUT2, OUT3, and OUT4 with respect to port IN1.

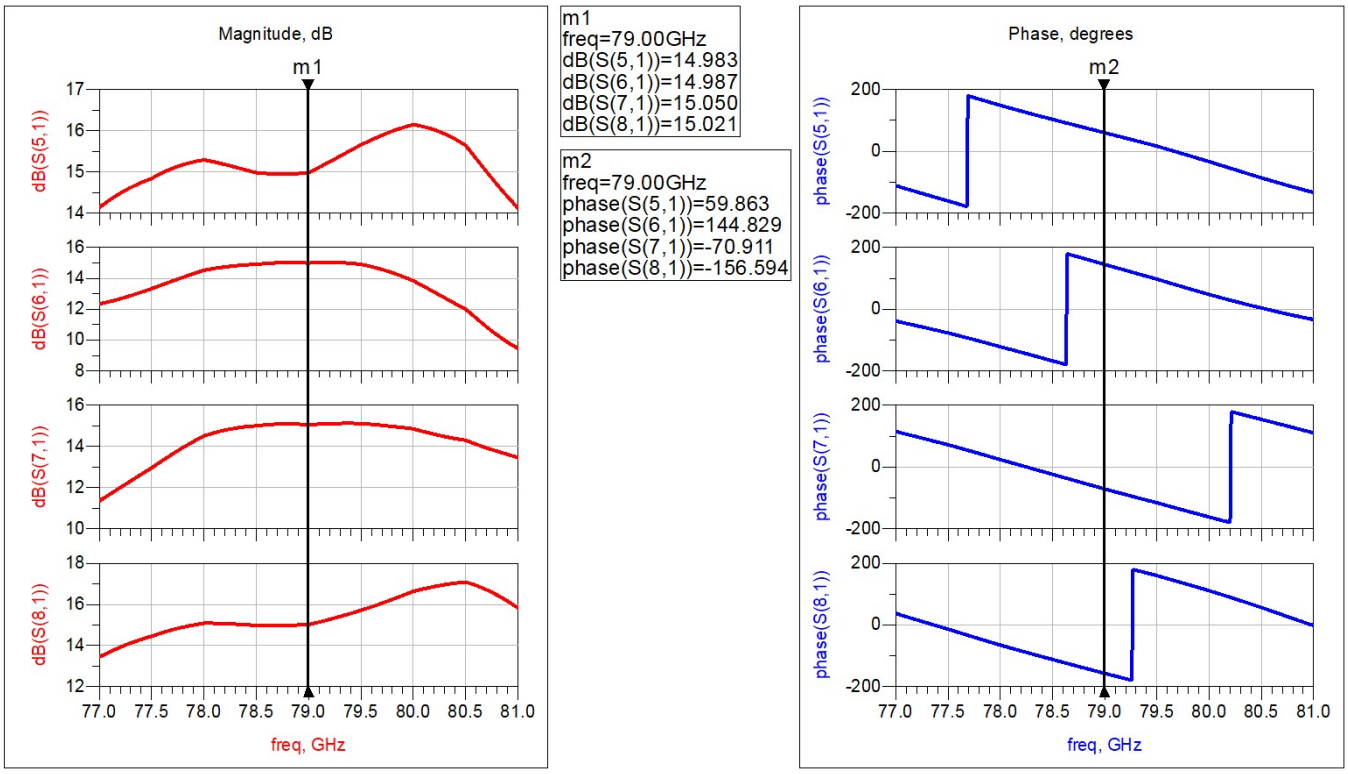

Figure 48: Balanced Four Port Power Phase Simulation Results

9.7 Output Power Summary

Table 13 below summarizes the power distribution in terms of output port as well as relative phase lags of each phase shifter. Let, $\Phi_n \propto$ the phase shift of TLn where n is lines 1 through 4. Reference Figure 37 for visual illustration of phase shifter (microstrip transmission line) locations.

Table 13: Phase Shifting and Output Power Summary

Focused Output Port	Φ_1 (°)	Φ_2(°)	Φ_3(°)	Φ_4(°)	Gain (dB)	P_{out} (W)
OUT1	22.2791	184.0740	222.7910	61.2872	20.04	100.9253
OUT2	222.8160	55.5845	22.2816	180.9520	19.9	97.7237
OUT3	33.9259	24.9696	208.3800	211.1930	20.993	125.6898
OUT4	34.1722	25.1538	28.0033	32.9865	20.996	125.7766
All, balanced	208.3400	207.8890	32.5156	214.5210	*	**

$*$ Balanced gain (dB) for each port [1, 2, 3, 4] = [14.983, 14.987, 15.050, 15.021]
$**$ Balanced P_{out} (W) for each port [1, 2, 3, 4] = [31.4992, 31.5283, 31.9890, 31.7761]

Note the P_{out} parameter in Table 13 is assuming a 0dB input signal converting the gain parameter to linear power, in units Watts. Additionally, the listed gain values are *excluding* the 3.2dB antenna gain.

10 Conclusion

This project resulted in the successful design of a Multiport Amplifier and Antenna system. All of the initial design specifications listed in Table 1 were achieved. At the center, design frequency the single port focused output gain was maximized to approximately 21 dB, while the balanced, four port output gain averaged 15 dB. With a 0 dB single input reference, the single port, focused output power is approximately maximized to an exceptional 126 W while a balanced, four port output power yielded approximately 31 W. The system also met DC power requirements by only consuming 520 mW. The final specification that was achieved was the TX Signal Direction. Table 1 requires the system to cover a radiated area of -50 to +50 degrees orthogonal to the antenna. Referencing Section 8, Figure 35 shows the antenna effective radiation area covering a full 180° orthogonal to the antenna. Arranging the four patch antennas in parallel to each other increases the full effective radiation area to the left and right of the entire system yielding a full -90 to +90 degree coverage, orthogonal to the antennas (and system), satisfying the initial -50 to +50 degree TX Signal Direction specification. Furthermore, it's worth noting *all the dimensions of each component designed and the full system itself were physically realizable.* A full system layout extracted from the ADS Layout terminal can be observed below in Figure 49.

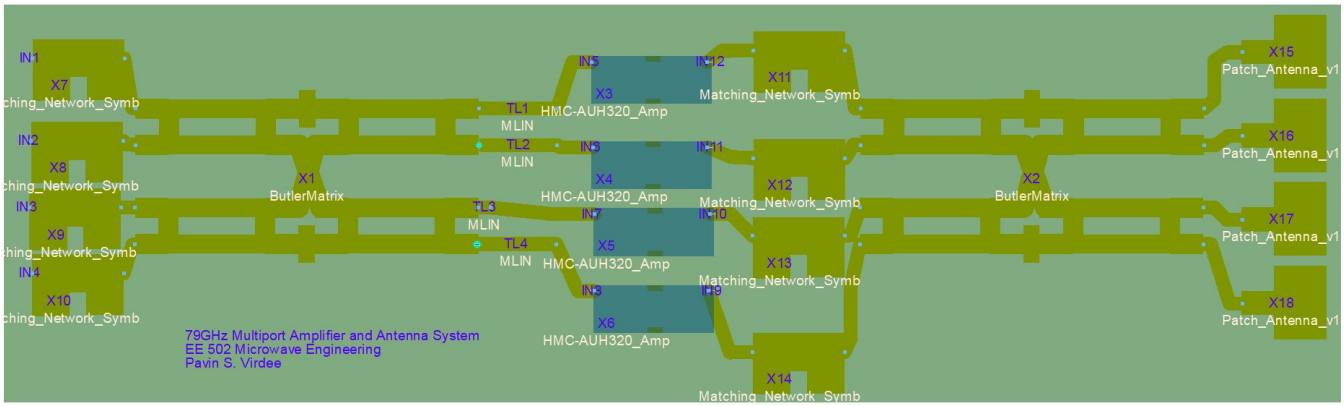

Figure 49: Full System Layout via ADS Layout Terminal

Figure 50 also illustrates the extracted Gerber files via a Gerber file viewer (*via gerber-viewer.com*).

Note, the final design dimensions were 960 $mils \times 285$ $mils$.

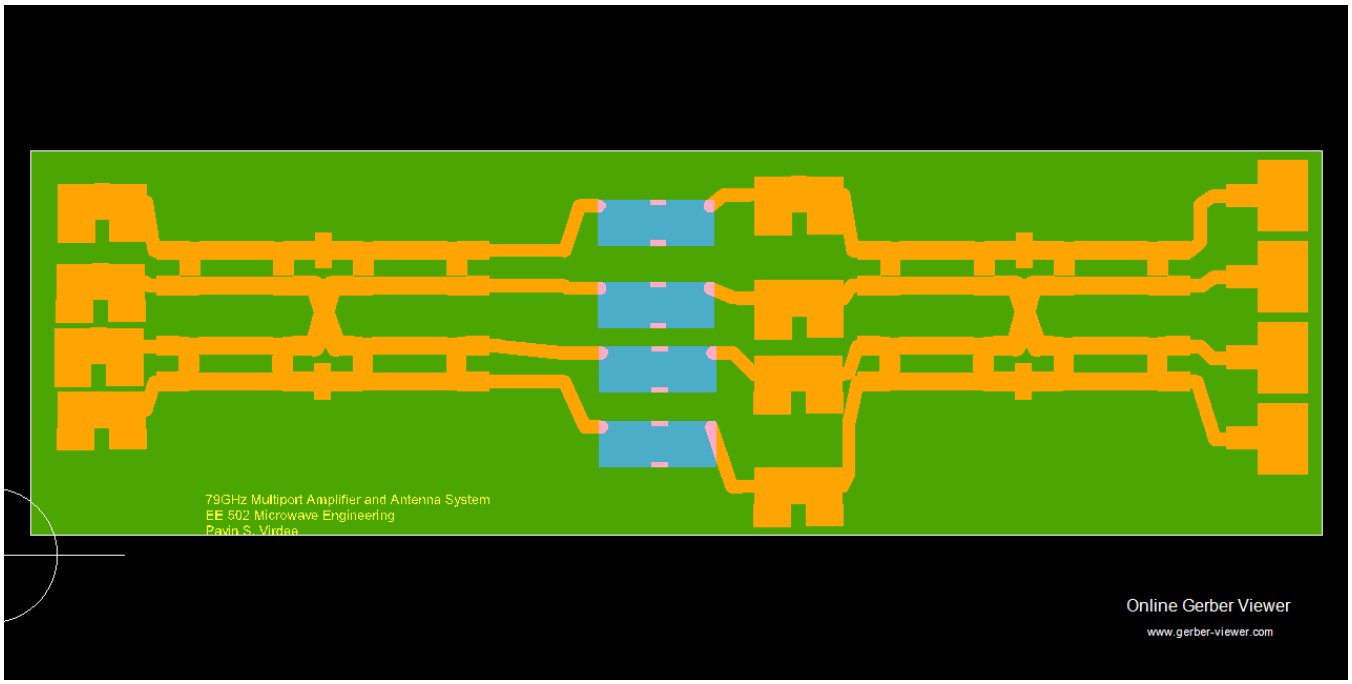

Figure 50: Extracted Gerber Files Layout View

In conclusion, a lot was accomplished with this project within the *relatively* short time frame. An immense amount of experience with Keysight ADS was acquired as well as a great deal of practical and conceptual knowledge. Moreover, it was extremely challenging designing RF components and a full system at such a high millimeter wave frequency, but in-turn yielded a great learning experience.

To further expand on this project, more can still be accomplished down the line if it were to be picked up for future research and projects. Automated or digitally controlled phase shifters can be implemented, a full system hardware layout implementation can be developed by integrating the HMC-AUH320 amplifiers and fabricating the board, better antennas can be designed, beam steering optimization and testing can be performed, and further general design optimization can be performed.

Acknowledgements for this project would like to be given to Dr. Dennis Derickson along with Kyle Woolrich of Boeing Company. Kyle gave the Microwave Engineering class an in-depth presentation regarding MPA's that served as good background for this project. Dr. Derickson provided an abundance of resources and support to help develop this project as well. Overall, this project was very fascinating and I enjoyed the challenge of designing this system at 79 GHz. *All things considered, this project may be a favorable option for Master's Thesis selection in the coming year.*

References

[1] D. M. Pozar, Microwave Engineering. Wiley, 2012.

[2] Dr. P.J. Bevelacqua, "Antenna Theory Encyclopedia." https://www.antenna-theory.com/, 2021.

[3] Analog Devices, "GaAs HEMT MMIC Medium Power Amplifier, 71-86 GHz." https://www.analog.com/media/en/technical-documentation/data-sheets/hmc-auh320.pdf, 2012.

[4] Rogers Corporation, "RO3000 Series Circuit Materials, High Frequency Laminates." https://rogerscorp.com/-/media/project/rogerscorp/documents/advanced-connectivity-solutions/english/data-sheets/ro3000-laminate-data-sheet-ro3003-
pdf, 2019.

[5] Texas Instruments, "Moving from legacy 24 GHz to state-of-the-art 77 GHz radar." https://www.ti.com/lit/wp/spry312/spry312.pdf?ts=1613451431080&ref_url=https%253A%252F%252Fwww.google.com%252F, 2017.

[6] everythingRF Encyclopedia, "RF/Microwave White Notes and Application Notes." https://www.everythingrf.com/whitepapers, 2021.

[7] Keysight Technologies, "Creating Hierarchical Designs." https://edadocs.software.keysight.com/display/ads2009/Creating+Hierarchical+Designs, 2009.

[8] Microwaves101 Encyclopedia, "Microwave Encyclopedia." https://www.microwaves101.com/, 2021.

[9] Keysight Technologies, "Momentum Key Features." https://www.keysight.com/us/en/lib/resources/training-materials/momentum-key-features-1936424.html, 2020.

[10] A. Mallet, A. Anakabe, and J. Sombrin, "Multiport-amplifier-based architecture versus classical architecture for space telecommunication payloads," pp. 4353–4361, 2006.

[11] Microwave Journal, "Multiport Power Amplifiers for Flexible Satellite Antennas and Payloads." www.microwavejournal.com/articles/9430-multiport-power-amplifiers-for-flexible-satellit
2010.

[12] I. Soga, Y. Yagishita, H. Matsumura, Y. Kawano, T. Suzuki, and T. Iwai, "A 76–81 ghz high efficiency power amplifier for phased array automotive radar applications," in 2015 IEEE International Symposium on Radio-Frequency Integration Technology (RFIT), pp. 166–168, 2015.

A Double-Stub Tuner Design MATLAB Source Code

```
function [L1,L2] = dstMatchingDesign(Gmag,Gphi,d,stub,Zo)
% function [L1,L2] = dstMatchingDesign(G_mag,G_phi,d,stub,Zo)
% This function finds the two lengths L1 and L2 of either open or
% short circuit stubs for a double stub tuner matching network design.
% Input Parameters:
%   Gmag = Magnitude of the Reflection Coefficient to match
%   Gphi = Phase Angle in degrees of the Reflection Coefficient to match
%   d = set intermediate series stub between shunt stubs
%   stub = either 'open' or 'short' circuit shunt stubs
%   Zo = Characteristic Impedance of System
% Output Parameters:
%   L1 = length of the first shunt stub nearest the Load Match terminal
%   L2 = length of the second shunt stub nearest the pre-matched Zo/Yo
%        terminal
% NOTE:
%   d, L1, L2 are in terms of electric length & are the coefficient values
%   that get scaled by lamnda (wavelength)
% By: Pavin Virdee
clc; close all;

Yo = 1/Zo;      %Characteristic Admittance
Gamma = Gmag*exp(1i*Gphi*pi/180);   %complex form of the reflection coef.
yL = (1-Gamma)/(1+Gamma);           %Normalized Load admittance
YL = yL*Yo;                         %Load admittance
GL = real(YL);                      %Load conductance
BL = imag(YL);                      %Load susceptance

t = tan(2*pi*d);    %tangent term of the intermediate series stub
                    %should be tan(beta*d), but the lambda's will cancel
                    %and just leave 2pi*d

%susceptance of the first shunt stub nearest the Load
B1 = -BL + ((Yo + sqrt((1+t^2)*GL*Yo-GL^2*t^2))/(t));

%susceptance of the second shunt stub nearest the pre-matched Zo terminal
B2 = (Yo*sqrt(Yo*GL*(1+t^2)-GL^2*t^2)+GL*Yo)/(GL*t);

open = 'open';  %pre-defining open value for conditional check below
if stub == open
    L1 = 1/(2*pi)*atan(B1/Yo);  %length L1 in terms of electric length
    L2 = 1/(2*pi)*atan(B2/Yo);  %length L2 in terms of electric length
%if not open then must be short
else
    L1 = -1/(2*pi)*atan(Yo/B1);  %length L1 in terms of electric length
    L2 = -1/(2*pi)*atan(Yo/B2);  %length L2 in terms of electric length
end

%print shunt stub lengths to command window
disp(['L1 = ',num2str(L1),' *lambda']);
disp(['L2 = ',num2str(L2),' *lambda']);

end
```